Stockholm University

# Bachelor Thesis

**Degree Project in Marine Geology 15 hp**

# A distal signal of the Gold Cove glacial event in Bonavista Bay, Newfoundland

James Williams

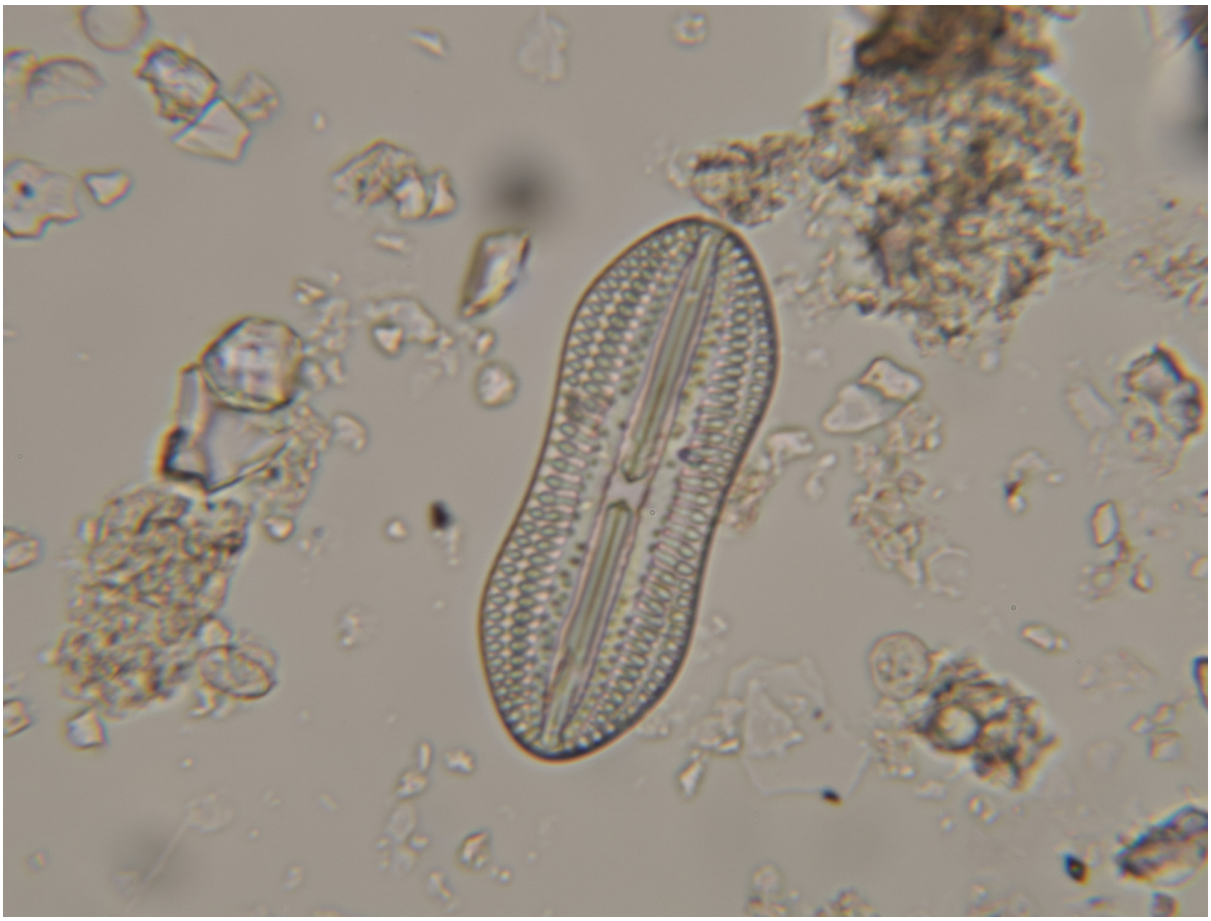

Stockholm 2015

Department of Geological Sciences
Stockholm University
SE-106 91 Stockholm

**Abstract**

The gradual demise of the Laurentide ice sheet was punctuated by a series of abrupt re-advances, and subsequent retreats, along its eastern margin. These advances of the glacial margin are associated with the release of large volumes of meltwater to the North Atlantic, and the deposition of detrital carbonate layers within the Labrador Sea. Furthermore, the sudden flux of meltwater is thought to perturb ocean circulation and have been implicated in northern hemisphere climate change throughout the Holocene. Here, using the marine sediment core AI07-01G, recovered from Bonavista Bay, Newfoundland, we apply a multi-proxy approach to investigate the local oceanographic conditions and ice margin processes during the Gold Cove retreat phase of the Laurentide ice sheet. Our results show a coeval increase in $CaCO_3$, Ca/Sr and silt sized grains at ca. 10.4 cal ka BP. We also observe an increase in the Arctic water diatom species *Thalassiosira gravida*, *Thalassiosira kushirensis* and *Bacterosira bathyomphala*. We suggest that the retreating margin of the Laurentide ice sheet was characterised by the formation of turbid plumes of meltwater and icebergs by claving, which transported detrital carbonate to the distal Newfoundland shelf. Furthermore, increased fresh water flux to the Labrador Sea resulted in the increasing of the strength of the Labrador Current, bringing colder surface waters and increased Arctic Water diatom species to sub-Arctic localities.
**Keywords:** Detrital Carbonate; Gold Cove Retreat; Labrador Current; Laurentide Ice Sheet; Turbid plume

# Contents

**Abstract** **3**

**1 Introduction** **6**
1.1 Glacial advance and retreat of the Laurentide ice sheet . . . 7
1.2 The Gold Cove advance and retreat . . . 7
1.3 Study site . . . 9
1.3.1 Bonavista Bay . . . 9
1.3.2 Ocean circulation . . . 10
1.3.3 Atmospheric circulation . . . 10

**2 Materials and methods** **12**
2.1 Chronology . . . 12
2.2 Diatoms . . . 13
2.2.1 Sample preparation . . . 13
2.2.2 Diatom taxonomy and enumeration . . . 13
2.3 Grain size analyses . . . 14
2.4 Geochemical analyses . . . 14

**3 Results** **15**
3.1 Chronology . . . 15
3.2 Grain size analyses . . . 15
3.3 Geochemical analyses . . . 17
3.4 Diatoms . . . 18

**4 Discusion** **22**
4.1 Retreat of the Gold Cove glacial event . . . 22
4.2 Transport of detrital carbonate during the Gold Cove retreat . . . 22
4.3 Increased strength of the Labrador Current during the Gold Cove Event and increased Arctic input . . . 24
4.4 The biogenic repsonse to glacial retreat . . . 25
4.5 Implications . . . 25
4.6 Limitations . . . 25
4.6.1 Chronology . . . 25
4.6.2 Diatoms . . . 26
4.6.3 Grain size analyses . . . 26
4.7 Future work . . . 26

**5 Conclusions** **28**

**References** **30**

**Appendices** **36**

# List of Figures


1 The Gold Cove advance . . . . . 8
2 Annual variability in temperature, sea ice and salinity within Bonavista Bay . . . . . 9
3 Oceanography of the Labrador Sea . . . . . 11
4 NAO and sea ice advection in the Labrador Sea . . . . . 12
5 AI07-01G age model . . . . . 16
6 Results - coarse sand ($> 250$ $\mu$m and XRF Ca . . . . . 17
7 Results - geochemical and grain size analyses . . . . . 19
8 Diatom abundances . . . . . 21
9 Ice margin plumes . . . . . 23

# 1 Introduction

Throughout the Pleistocene, Canada and the interior plains of North America were dominated by the large, dynamic, Laurentide ice sheet. Following its maximum extent ca. 18 cal ka BP (calibrated thousand years before 1950), the decline of the Laurentide Ice Sheet (LIS) was punctuated by a series of re-advances along its eastern margin during the early Holocene Each advance and retreat of the ice sheet resulted in the release of large volumes of glacial meltwater to the North Atlantic, in the form of icebergs predominantly through Hudson Strait (Bond et al., 1992; Andrews et al., 1993; Rashid et al., 2011).

It has been suggested that large fluxes of freshwater to the North Atlantic, associated with the decline of the Laurentide Ice Sheet (LIS) have far reaching implications, affecting climate in Europe by tele-connections (Broecker, 1994). For example, the 8.2 ka final drainage of glacial Lake Agassiz is thought to have perturbed the North Atlantic thermohaline circulation significantly, resulting in a 4°C cooling over Greenland and 1.5°C cooling of North Atlantic sea surface and surrounding continental areas (Barber et al., 1999; Wiersma and Jongma, 2010).

Therefore, an understanding of the timing and extent of glacial meltwater release is imperative if excursions in oceanic and terrestrial climate records are to be correlated, and potential forcing mechanisms constrained. As such, the identification of the marine signature of glacial advances can be used to constrain the timing of, and oceanographic changes during glacial readvance/retreat cycles, and their impact on the global climate system.

The focus of research has been concentrated on the more prominent, ocean crossing Heinrich Events (Bond et al., 1992; Hemming, 2004). However, recent interest has turned to the series of glacial margin readvances during the early Holocene, such as the Gold Cove and Noble Inlet glacial events (Manley and Miller, 2001; Rashid et al., 2014; Jennings et al., 2015).

The study of marine sediments has focused mainly on sites proximal to Hudson Strait, or where further, in the Orphan Basin (Rashid et al., 2014; Jennings et al., 2015). Foraminiferal $\delta^{18}O$ and grain size changes are most often invoked for reconstructing ocean changes during these events. In this study, however, we investigate the response of diatom assemblages during one of these glacial events. Diatoms are marine phytoplankton, carrying out photosynthesis. Diatoms are useful as proxies of sea surface conditions because they restricted to the photic zone of the water column, are abundant, and form siliceous frustrules that are often well preserved in the fossil record. Furthermore, the majority of species observed throughout the Holocene extant, and their ecological ranges well constrained (Julius and Theriot, 2010). As such, diatom studies have been used to reconstruct sea surface conditions, using transfer functions for example, in the Arctic and Antactica, as well as playing a fundamental role in the reconstruction of sea surface temperatures during the last glacial period (Gersonde et al., 2005; Leventer et al., 2010)

The Newfoundland shelf is a prime location to study glacial advance and retreat events due to its position south of Hudson Strait. Any Icebergs or melt water moving south into the North Atlantic are assumed pass over the shelf and leave some signature in the sedimentary record. The sediment core AI07-01G affords us an opportunity to investigate the a glacial retreat, the Gold Cove retreat, within the Labrador Sea in high resolution. Sites this far south investigating meltwater have focused on changes in the Orphan knoll basin, bathed by the outer Labrador Current (i.e. Rashid et al., 2014) as opposed to changes observed in the inner Labrador Current and shelf region.

Here, we investigate sediments containing increased detrital carbonate in core AI07-01G from Bonavista Bay, Newfoundland using a multi-proxy approach. We combine sedimentological (grain size) and geochemical proxies (XRF Ca and Sr, TOC, and $CaCO_3$), as well as diatom assemblage counts to reconstruct the mode of transport and deposition, as well as changes in marine surface conditions during the early Holocene. The specific objectives of this study are to (i) constrain the

timing of the Gold Cove Event in this distal region of the Labrador Sea; (ii) investigate the changes in lithological proxies, and relate them to a mode of transport and deposition for detrital carbonate during the retreat phase of the glacial margin; (iii) investigate changing surface water conditions i.e temperature, salinity, using diatom assemblage counts; and (iv) discuss the implications of these glacial events on local productivity and hydrography.

## 1.1 Glacial advance and retreat of the Laurentide ice sheet

Hudson Strait was the principal drainage route for the majority of the LIS during the last glaciation (Andrews and Tedesco, 1992; Bond et al., 1992; Broecker et al., 1994). Hudson Strait is underlain by Ordovician carbonates (Miller and kaufman, 1990). Erosion of the floor of Hudson Strait during glacial readvances resulted in the entrainment of high concentrations of carbonate within the ice stream. Consequently, high volumes of detrital carbonates are released to the Labrador Sea during calving and meltwater events (see review by Hemming, 2004). Whilst early Holocene detrital carbonate events (DCE) are analogous to the North Atlantic spanning Heinrich events, it should be noted that early Holocene DCEs occur on a considerably smaller scale, with deposits confined to the Labrador Sea, and hence a distinction is made in terminology (detrital carbonate event).

Pulses of detrital carbonate are associated with readvance and subsequent collapse of the Laurentide Ice Sheet and the early Holocene sediments along the Labrador Shelf also received massive inputs of detrital carbonate between 8-9 $^{14}$C ka BP (Andrews et al., 1999). At ice proximal locations these DCEs are characterised by the presence of massive clayey silts with little IRD and rich in carbonate, specifically calcite (Kirby and Andrews, 1999). The fine grained lithology associated with calving of the LIS suggests that in these ice margin proximal regions, deposition was associated with large volumes of meltwater, in the form of turbidity flows and hyperpycnal plumes, (Rashid et al., 2014) and surface meltwater plumes (Hillaire-Marcel et al., 1994; Hesse et al., 1997). These observations suggest that DCEs are associated with the generation of massive amounts of meltwater at the bed of the ice stream. Furthermore, geochemical studies of planktonic foraminifera $\delta^{18}$O suggest that increased meltwater flux lead to significant decreases in surface water salinity (Andrews at al., 1994). Accompanying the dominance of calcite is a decrease in magnetic susceptibility due to the diamagnetic properties of calcite (Andrews and Tedesco, 1992).

## 1.2 The Gold Cove advance and retreat

The Laurentide Ice Sheet (LIS) dominated northern Canada during the last glaciation, being centred over the interior marine basins of Hudson Bay and Foxe Basin and connected to the North Atlantic via Hudson Strait (Kaufman et al., 1993). The Labrador sector of the LIS was the largest dome of ice during the early Holocene, covering an area of 3,000,000 km and reaching >2 km at its thickest (Kaufman et al., 1993; Clarke et al., 2000). The Gold Cove advance (GCA) represents the largest northward advance of Labrador sector ice during the deglaciation of the LIS (Veillette et al., 1999).

During the Gold Cove event, the Labrador ice margin advanced 300 km north across the mouths of the Hudson Strait and Frobisher Bay. At its maximum extent, the ice margin crossed considerable topography, overrunning summits of ca. 400 m above sea level before reaching the southern margin of Baffin Island and extending offshore to Hall Peninsula (Figure. 1) (Miller and Kaufman, 1990; Kaufman et al., 1993; Veillette et al., 1999). The maximum extent of the surging ice is well constrained by cross-cutting striations, erratic emplacement and the deposition of carbonate drift derived from the floor of Hudson Strait (Kaufman et al., 1993; Andrews et al., 1995). As a result, glaciomarine conditions persisted along the eastern margin of the ice sheet and in the Hudson Strait region (Andrews et al., 1995). These glaciomarine conditions resulted in an estimated 300 km$^3$ a$^{-1}$

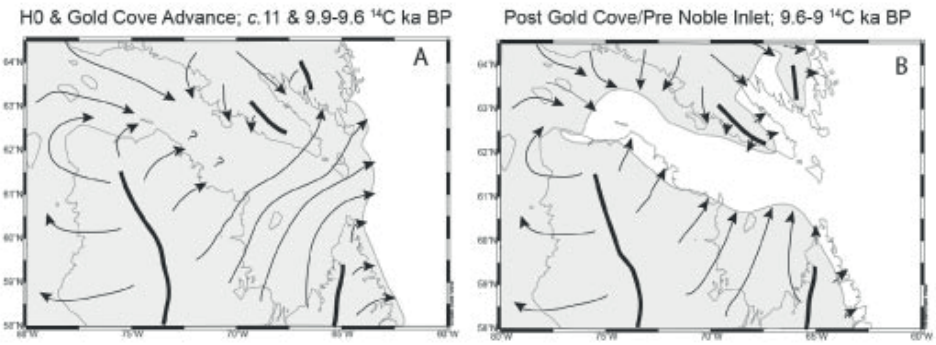


Figure 1: The extent of the Laurentide ice sheet prior to, and after the Gold Cove advance. Arrows indicate the ice flow direction. During the advance stage, ice is observed as flowing from the Labrador-Ungava area, across the axis of the Hudson Strait and extending to Hall Peninsula. After Manley and Miller, (2001)

of calving >200 km into open water, 500 m deep, sustained by high flow velocities (Veillette et al., 1999).

The age of the Gold Cove advance is well constrained by over 60 radiocarbon dates obtained from marine molluscs, including 27 AMS $^{14}$C dates on single specimens (Kaufman et al., 1993). The glacial advance was rapid, occurring within 200 radiocarbon years, with the maximum extent of ice reached between 9.9-9.6 $^{14}$C Ka BP. The retreat phase of the Gold Cove event was similarly short lived, also lasting only 200 radiocarbon years. However, the ice margin retreated some 350 km (Manley and Miller, 2001). Recently, the age of this surge and retreat has been the topic of considerable debate. Rashid et al, (2014) propose that the date of the advance stage, corresponds to 10.2 cal ka BP. However, Pearce et al, (2015) argue that the advance occurred much earlier, between 10.6-11 cal. ka BP.

The cause of the surging ice is not well constrained. Miller and Kaufman, (1990) suggest that increased precipitation during the Younger Dryas (as recorded in the GISP 2 ice core) considerably thickened the Labrador ice dome, result in the binge and basal sliding as a consequence of warming (MacAyeal, 1993). Alternatively, Clark et al, (2000) argue that previous activity of the Hudson Strait ice stream (specifically during H0, ca. 11 Ka) resulted in the destabilisation of the Labrador ice dome toe, promoting strain heating and headward growth as a result.

Calving during the maximum extent and retreat of the ice margin would have had several consequences such as increasing sea level (Fairbanks, 1989; Tornqvist and Hijma, 2012). Furthermore, estimates of calving losses of 300 km$^3$ a$^{-1}$ are close to that required to affect thermohaline circulation (Rahmstorf, 1995). As such, the Gold Cove event has been invoked as the driving mechanism of observed cooling of the Nordic Sea and air temperatures over Greenland (Lehman and keigwin, 1992; Koc Karpuz and Jansen, 1992; Johnsen et al., 1992).

A detrital carbonate layer corresponding in age to the Gold Cove event has not been observed in the North Atlantic region as with the larger scale Heinrich events (Bond et al., 1992). It is likely that warm poleward flowing Atlantic waters resulted in the melting of icebergs before they reached the North Atlantic Ocean. Miller et al, (2001) suggest that with the return of a stronger overturning circulation and southward shift of the atmospheric polar front to near modern position, icebergs would have been restricted to the Labrador shelf region, tracking southward instead of east. Possibly resulting in minimal effect on the circum-Atlantic current. However, it has been suggested

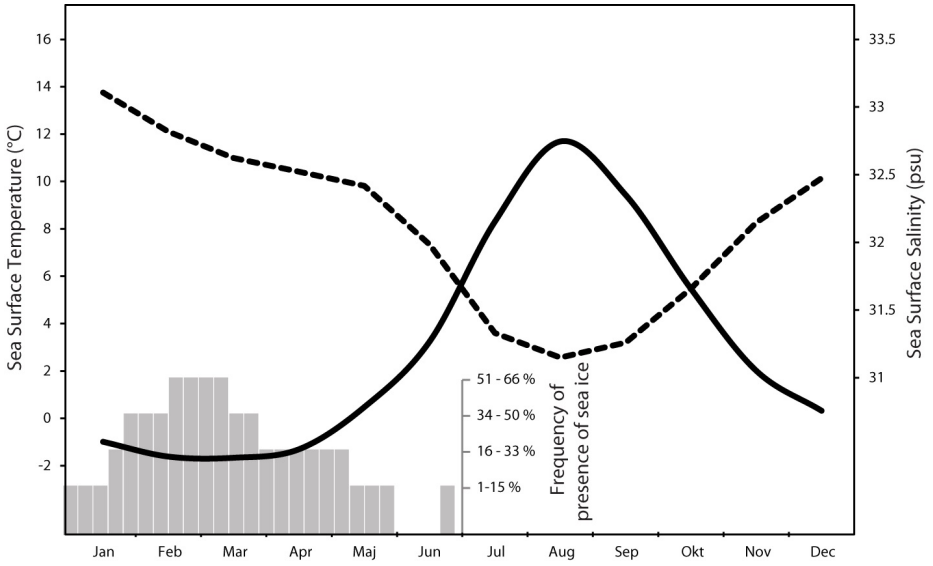


Figure 2: Changing sea surface temperature (solid line) and sea surface salinity (dashed line) throughout the year at Bonavista Bay. The histogram shows the weekly frequency of sea ice. Sea ice can be observed as late as June, when temperatures begin to rise considerably and salinity decreases. Modified after Pearce et al, (2014).

that due to the modern-like arrangement of ocean currents in the region, detrital carbonate from the event did not extend into the deep North Atlantic due to it being confined to the Labrador Current (Dyke et al., 1996)

## 1.3 Study site

### 1.3.1 Bonavista Bay

Bonavista Bay is a broad embayment (65 km wide) located on the northeast coast of Newfoundland, situated between Cape Freels in the northwest, and Cape Bonavista in the southeast (Figure. 2). The western margin of the bay contains a series of narrow fjords, connected to the outer bay by shallow sills (Cumming et al., 1991). An elongate depression, Central Basin, marks the deepest area of the bay, exceeding depths of 450 m. The bay also contains a number of densely forested islands which shelter the mainland from northeasterlies. Cumming et al, (1991) suggest that a grounded ice sheet extended offshore during the last glacial maximum (ca. 20 $^{14}$C ka). The deglaciation of the bay lasted until ca. 10 $^{14}$C ka, resulting in the deposition of outwash and the establishment of normal marine conditions throughout the bay.

The climate of Bonavista Bay is classified as mid-boreal and extremely sensitive to seasonality. Mean air temperatures range from -4 °C in January and 16 °C in July (figure 2). Sea surface temperatures range from -2 °C to 12 °C and sea ice annually covers Bonavista Bay from January until April or May (Canadian Ice Service, 2013). The sea ice is most often advected from localities north of 68°, such as Baffin Bay, Davis Strait and West Greenland, but occasionally forms locally (Deser et al., 2002).

### 1.3.2 Ocean circulation

The residual circulation in the Labrador Sea is mainly cyclonic, consisting eddies in its interior (Prater, 2002) and the Labrador Current along the western Boundary (figure 3). The Labrador Current is responsible for the transportation of two thirds of the low density freshwater transport from the Arctic to the North Atlantic and subsequently mid latitudes (Aksenov et al., 2010). The Labrador Current is also responsible for the advection of sea ice from higher latitudes including Baffin Bay and the west coast of Greenland (Drinkwater, 1996; Petrie, 2007).

The Labrador Current is composed of inputs of the warm West Greenland Current, the cold Baffin Island Current, as well as glacial meltwater from Greenland and the Canadian Arctic Archipelago. Upon reaching the Davis Strait (ca. 66°N), the West Greenland Current, carrying warm Atlantic water, splits into two branches. The first, and main, branch crosses the Labrador Sea where it mixes with water from Baffin Bay, forming the warmer, higher salinity Outer Labrador Current (4 °C, 34.5 ‰) which flows southward along the edge of the continental slope, carrying 80% of southbound waters (Vilks, 1980; Drinkwater, 1996). The outer LC flows southeast over the Newfoundland shelf before reaching the Flemish Cap and the Grand Banks where some retroflects northward upon encountering the North Atlantic Current (NAC) (Fratantoni and McCartney, 2010), but the majority continues southward along the eastern slope to the tail of the Banks.

The hydrography of Bonavista Bay is directly influenced by the Inner Labrador Current, the coastal branch of the Labrador Current, a boundary current characterised by low temperature and low salinity. The second branch of the WGC continues northward to Baffin Bay, where it joins the southward-flowing Baffin Island Current which contains low-salinity Arctic water. This current is supplemented by riverine outflow from Hudson Bay which is mixed with deep water within Hudson Strait as a result of strong a tidal regime to the form the colder, Inner Labrador Current ($0-2$ °C, 31-33‰) (Lazier and Wright, 1993; Mertz et al., 1993; Drinkwater, 1996; Loder et al., 1998). The Inner Labrador Current flows through the Avalon Channel off east Newfoundland (Petrie and Anderson, 1983; Petrie and Isenor, 1985) and continues westward toward the Gulf of St. Lawrence. Along its path, the Labrador Current has little exchange with the central Labrador Sea due to steep salinity gradients.

### 1.3.3 Atmospheric circulation

Newfoundland is situated in an atmospheric frontal zone where cold westerly winds from the Arctic predominate, caused by the interaction of atmospheric low over Canada, and highs over Bermuda and the northeast Pacific. The strength of these westerlies is strongly influenced by the North Atlantic Oscillation (NAO) (figure 4). When the NAO index is positive, (corresponding to a large difference in atmospheric pressure between the Azores Islands and Iceland) westerly winds are strongest during the winter months (Drinkwater, 1996; Weckstrom et al., 2013). Drinkwater (1996) observe that air and sea surface temperatures are lower during periods of positive NAO index, i.e. when regional westerly winds are strongest. The positive NAO index also results in increased advection of sea ice and low salinity anomalies from adjacent regions (Prinsenberg et al., 1997; Deser et al., 2002). Conversely, when the NAO index is negative, wind strength is significantly reduced over the region. The weakest winds are observed in summer and blow as south westerlies.

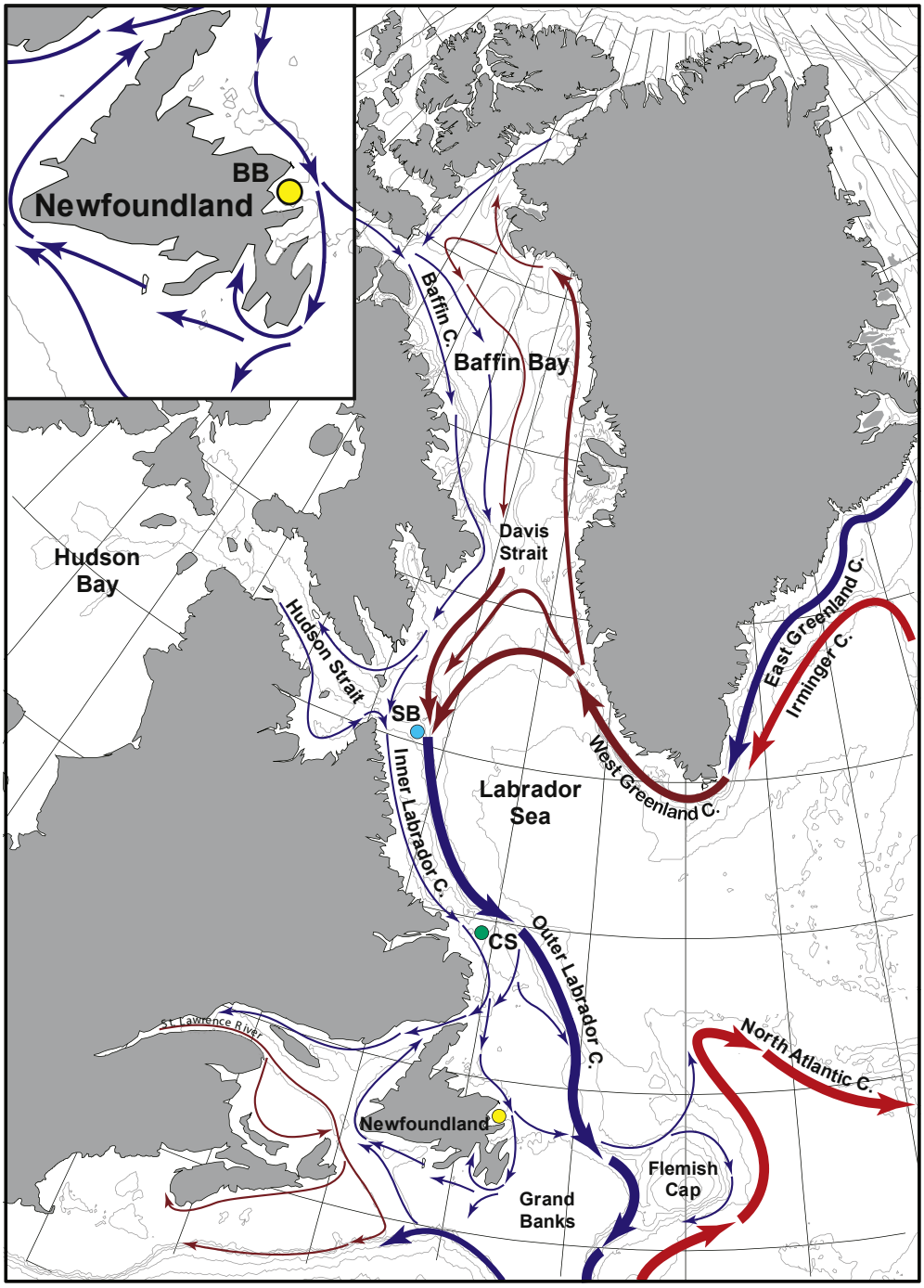


Figure 3: The oceanographic circulation within the Labrador Sea. Warm currents are marked as red, cold as blue. Intermediate currents are marked as dark red (burgundy). The location of Bonavista Bay is shown as the yellow circle. Cartwright Saddle and Sagalek Bank (see discussion) are marked as green and blue circles respectively. After Weckström et al., (2013).

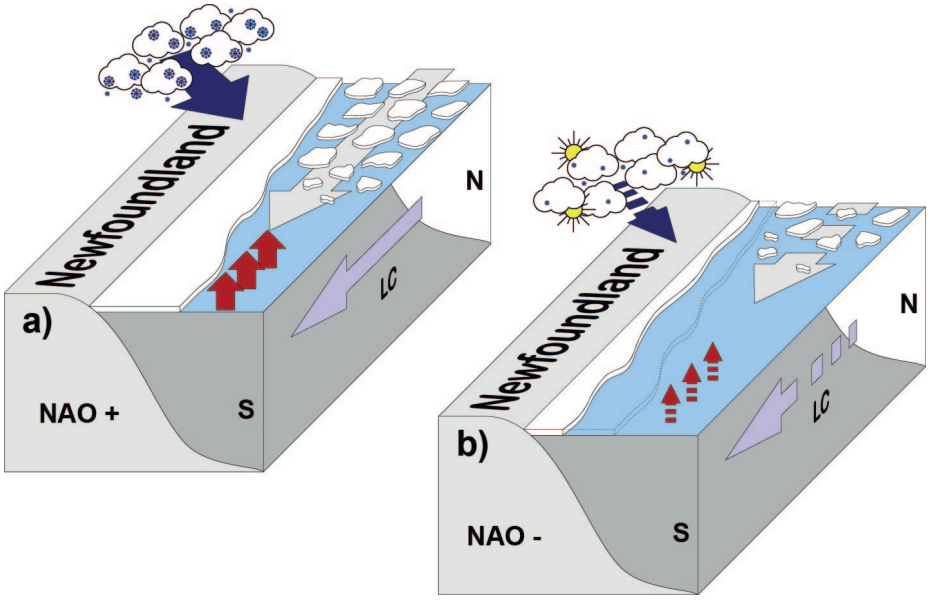


Figure 4: The affect of NAO index on sea ice advection in the Labrador Sea. During negative years, westerly wind strength and labrador current strength is reduced and less sea ice advected from northern latitudes to the coast of Newfoundland. The opposite is true for positive index years. Weckström et al, (2013).

# 2 Materials and methods

The marine sediment core AI07-01G was recovered from Bonavista Bay (48° 48.709'N, 53° 24.512'W, 317 m water depth) using a gravity corer from aboard the research vessel Akademik Ioffe on September $24^{[}th$, 2007. The coring process retrieved 557 cm of marine sediment from the seafloor, which was subsequently cut into 6 sections, and halved lengthwise to form working and archive halves as is standard practice. Core sections were stored at Aarhus University, Denmark at 2 °C in the absence of light to reduce the effects of diagenesis.

## 2.1 Chronology

In order to improve an existing preliminary age-depth model, calcareous samples were collected for radiocarbon dating at the Department of Geoscience, Aarhus University. Samples were collected from core AI07-01G on March $23^{rd}$, 2015 at depths of 95-100 cm and 151-155 cm respectively (sections 4 and 5). Samples were washed over a 100 $\mu$m sieve and allowed to dry at 40 °C for 8 h (grains in the 63-100 $\mu$m fraction size were retained for future analysis). Heavy liquid separation was carried out using tetrachloroethylene ($C_2Cl_4$) in order to separate the heavier sand particles from lighter foraminifera. Samples were dried in a fume hood for 8 h. Dry samples of the separated fraction containing foraminifera were analysed using a Nikon SMZ645 stereoscopic zoom microscope. Mixed benthic foraminifera species were used for dating due to the small size of the foraminifera, and weight requirement for dating. The species used for dating were *Elphidium bartletti*; *Elphidium excavatum*; *Globobulimina auriculata*; *Islandiella helenae* and *Nonionellina labradorica*. Where available marine mollusc shell fragments belonging to Yoldiella hyperborea were used in place of benthic foraminifera

species for convenience and improved dating accuracy. Samples were analysed at the AMS $^{14}C$ Dating Centre, Aarhus University.

The age-depth model was developed using the Oxcal v4.2.4 software (Ramsey, 2008). A total of 11 samples were calibrated using the Marine13 calibration curve by Reimer et al. (2013). A local marine reservoir age of 450 years ($\Delta R = 50 \pm 50$ years) was applied to the AI07-01G core in order to directly compare these data with those presented by Jennings et al, (2015). A constant $\Delta R$ is assumed throughout the core due to difficulties in quantifying potential reservoir changes.

## 2.2 Diatoms

### 2.2.1 Sample preparation

Samples were previously collected by Christof Pearce at Aarhus University in 2014 at 10 cm intervals throughout the core. At intervals of interest, samples were taken at higher resolution (ca. 2 cm). Samples were subsequently freeze dried and stored in at 2°C in the absence of light at Aarhus University.

Diatom slide preparation was carried out at the Department of Geological Sciences, Stockholm University between March $30^{th}$ and April $18^{th}$. No protocol for diatom sample preparation and microscope slide production had previously been established, so this research project includes some development of laboratory procedures. Sample preparation followed a modified version of the method presented by Warnock and Scherer (2014). Approximately 0.05g of freeze dried sediment were placed into 45 mL centrifuge tubes. Following this, 1 ml 10% HCl was added to the sample in order to remove carbonate material. Samples were incubated in a water bath at 80 °C for 1 hours in order to increase the reaction kinetics. Once the acid reaction was complete, 3 mL of 30% $H_2O_2$ was added and samples were incubated for an additional 3 hours in order to remove organic material.

Demineralized water was then added to the chemically treated sample until 45 mL of liquid was contained in the centrifuge tube. Samples were shaken so that diatoms were dispersed equally throughout the tube before 20 mL was pipetted into a customized sedimentation chamber containing a table with microscope cover glasses (Warnock and Scherer 2014). During pipetting care was taken to ensure an equal distribution of diatoms. Diatoms were allowed to settle through the water column for 6 h before the beakers were slowly drained through a tap at a rate of 2-3 drops $s^{-1}$. During this time beakers were covered to ensure no contamination or disturbance by air blowing across the water surface.

The purpose of this methodology is to equally distribute the diatoms across the cover glass surface such that the cover glass samples the whole flora without bias. Square beakers were used to reduce vorticity during draining, ensuring that settled diatoms were not remobilised. The duration of 6 h settling time was decided to allow sufficient time for diatoms to sink, whilst leaving clay particles suspended in the draining water column. These clay particles are removed during drainage, allowing for easier taxonomic identification. Coverslips were air dried and affixed to microscope slides using the high refractive index mountant Naphrax. A detailed, step-by-step instruction manual was written based on the outcome of the method development and will serve as a reference for future diatom laboratory work at the Department of Geological Sciences (see appendices).

### 2.2.2 Diatom taxonomy and enumeration

Diatoms were identified and counted across horizontal transects under X1000 magnification using a Leitz Labrolux 12 POL light microscope equipped with phase contrast optics. Photomicrographs were taken using a Nikon D5300 camera at the aforementioned objectives. Taxonomic identifications

were made with reference to Pearce et al, (2014), Hasle and Syvertsen (1997), Cremer (1998), Berard-Therriault et al (1999) and Witkowski et al. (2000). A total of 300 diatom valves were identified in each slide.

Diatom enumeration was carried out using a modified version the method presented by Zielinski (1993). Here, only whole valves or fragments containing both the pole and central area are counted. Using this protocol prevents counting of a single diatom valve twice. Due to their very high abundance, *Chaeteceros* resting spores were not included in the total count. Absolute diatom abundace (ADA) was calculated using the equation:

$$ADA = \frac{N \times At}{Ac \times m} \tag{1}$$

where $N$ is number of diatoms counted; $At$ is the surface area of the tray ($mm^2$); $Ac$ is surface area counted ($mm^2$) and $m$ is the dry mass of sediment used (g).

## 2.3 Grain size analyses

Grain size analysis was performed using the Mastersizer 3000 laser diffraction particle size analyser at Stockholm University during the period during the 4-6$^{th}$ May 2015. Samples were freeze dried in order to remove pore water prior to analysis. A small amount of the dried sample was broken off and gently crushed in order to homogenize the lithic material. This also avoids misdetection of aggregates of small grains, as larger (potentially IRD) grains. Background light scatter was measured for 15 seconds using blue light (470 nm) followed by 15 seconds of red light (632 nm).

Following background analysis, 3 ml of 10% sodium hexametaphosphate ($Na_6P_6O_{18}$ - Calgon) was added to the external Hydro LV wet dispersion unit. The purpose of the hexametaphosphate is to deflocculate and keep individual grains in suspension during analysis. Sample material was added until a suitable obscuration was achieved (between 5-10 % for samples from this core) and sonicated for 3 minutes. Analyses was carried out using the aforementioned blue and red light for 30 seconds at each wavelength. Five repeat measurements of each sample were made in order to improve statistical robustness of data. Repeat measurements of previously measured samples were also carried out every 5-10 measurements to observe any systematic drift in the analyser.

## 2.4 Geochemical analyses

Bulk geochemical composition throughout the core was carried out using the non-destructive Cortex x-ray fluorescence (XRF) core scanner at NIOZ, the Netherlands (Solignac et al., 2011). Analyses were performed at 10 kV in order to obtain semi quantitative elemental abundances of Ca and Sr Measurements were carried out at a resolution of 1 cm throughout the core. Calcium carbonate content (wt.%) was measured at the University of Copenhagen using the Metrohm 855 Robotic Titrosampler connected to a PC with Tiamo software. Approximately 1.0 g of sample was weighed into a 150 ml. Fifteen mL of 1.0 M HCl and approximately 100 mL of demineralized water was then added to the beaker. The mixture is subsequently boiled on a hotplate for 20 minutes and then titrated with 1.0 M NaOH until pH 7. Instrument accuracy is checked using pure $CaCO_3$ (100%) and the electrode is calibrated with buffer pH 4, 7 and 9. Total organic carbon (TOC%) was calculated following the calculation of total carbon (TC%) using the Eltra CS-500 C+S analyser connected to a PC. TOC was calculated using the formula:

$$TOC = TC\% - \frac{CaCO_3\% \times 12.01 \frac{g}{mol} C}{100.08 \frac{g}{mol} CaCO_3\%} \tag{2}$$

| Sample ID | Material | Depth range (cm) | Average depth (cm) | Radiocarbon age (yrs) | Error | ΔR | Calibrated age range ($2\sigma$) from | to | Modeled mean age (cal yr BP) | Error |
|---|---|---|---|---|---|---|---|---|---|---|
| AAR17525 | Mollusk fragment | 8 - 9 | 8.5 | 6943 | 30 | 50 ± 50 | 7514 | 7279 | 7404.5 | 63.8 |
| AAR18187 | Mollusk fragment | 41 - 42 | 41.5 | 7988 | 40 | 50 ± 50 | 8549 | 8274 | 8378.1 | 76.4 |
| AAR22314* | Mixed benthic foraminfera | 95 - 100 | 97.5 | 8496 | 37 | 50 ± 50 | 9260 | 8895 | 9014.2 | 101.7 |
| AAR22315* | Mollusk (*Y. hyperboria*) | 153 - 154 | 153.5 | 8685 | 34 | 50 ± 50 | 9443 | 9120 | 9293.2 | 94.4 |
| AAR18188 | Mollusk (unidentified) | 244 - 245 | 244.5 | 9420 | 37 | 50 ± 50 | 10403 | 10043 | 10164.5 | 95.2 |
| AAR17526 | Mollusk (*N. minuta*) | 314 - 315 | 314.5 | 8557 | 32 | 50 ± 50 | 10519 | 10216 | 10398.1 | 96.1 |
| AAR18189 | Mollusk (unidentified) | 321 - 322 | 321.5 | 9721 | 40 | 50 ± 50 | 10737 | 10381 | 10459.9 | 101.2 |
| AAR18190 | Mollusk (unidentified) | 403.5 - 404.5 | 404 | 9823 | 40 | 50 ± 50 | 10906 | 10516 | 10673.5 | 94.2 |
| AAR18191 | Mollusk (unidentified) | 456 - 458.5 | 457.25 | 9965 | 45 | 50 ± 50 | 11086 | 10681 | 10819.8 | 99.4 |
| AAR17527 | Mollusk fragment | 491 - 492 | 491.5 | 9986 | 34 | 50 ± 50 | 11094 | 10710 | 10902.6 | 100.4 |
| AAR18192 | Mollusk (unidentified) | 551 - 552 | 551.5 | 10096 | 40 | 50 ± 50 | 11193 | 10823 | 11065 | 88.1 |

Table 1: AI07-01G sample ages, depth and material. Samples AAR22314 and AAR22315 (shown here in red with an $*$ were collected during this study.

# 3 Results

## 3.1 Chronology

The age model of core AI07-01G (figure 5 and also table 1) ranges from 7,353 to 11,099 cal yrs BP with a mean error of ± 100 years. The age of the carbonate peak investigated herein ranges from 10,402-10,333 ± 100 cal yrs BP (depth 315-285 cm), with the peak maxima (as observed in XRF Ca) occurring at 10,374 cal yrs BP (307.5 cm). The older section of the core, corresponding to 11.1-10.1 cal ka BP (depths 240-557 cm, appears to consist of a constant sedimentation rate resulting in a high temporal resolution of ca. 3 yrs/cm. At depths shallower than 240 cm, temporal resolution is considerably lower at ca. 11 yrs/cm. However, it should be noted that this estimation of resolution is very rough given the number of changes in sedimentation rate across this section of the core. In any case, the vast majority of the core is able to be investigated at the sub-decadal scale.

## 3.2 Grain size analyses

Grain size analyses were carried out on a total 72 samples. We divide the grain sizes in fractions corresponding to clay (0-2 m); silt (2-63 $\mu$m); fine sand (63-250 $\mu$m); and medium-coarse sand (>250 $\mu$m). The clay particles show a small range of variability between 8% and 14%.

The abundance of clay particles decreases in the oldest section of the core from 11.1-10.6 cal ka BP (550-380 cm). There is a broad peak between 380-260 cm. Within this broad peak, the peak at 307 cm is observed as a small peak which corresponds to values ca. 13%. Smaller peaks, close timing/depth to this peak are not observed as a result of the broadness of the dominant peak. Following this broad peak, abundance steadily increases from 8% to 12%, before decreasing rapidly in the top 30 cm.

In contrast, there is greater variability in the silt fraction throughout the core, with large peaks above the background clearly discernible. Again, a steady decline in the amount of silt is observed in the core to a depth of 380 cm. However, peaks well above the trend variability are observed at

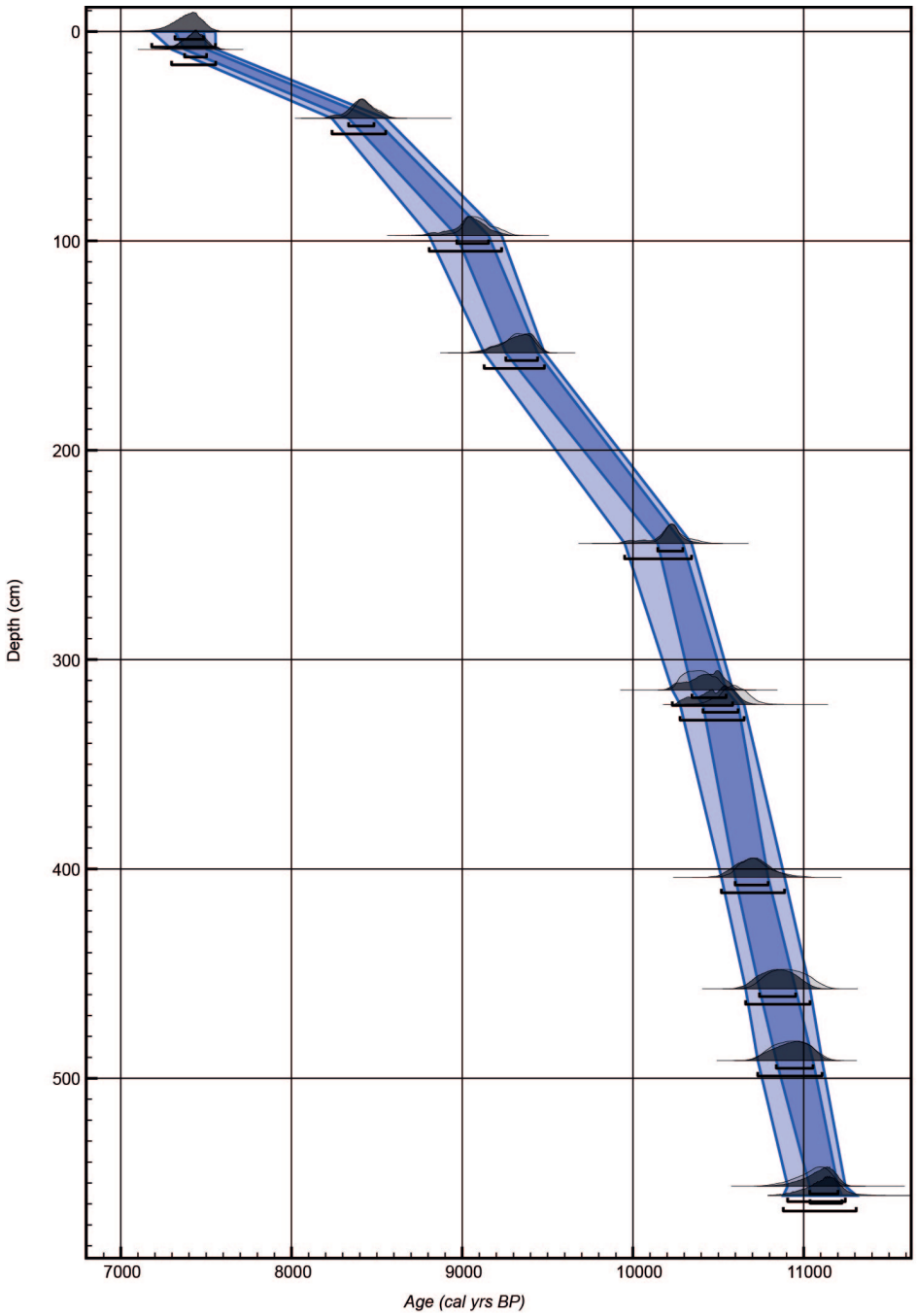


Figure 5: The AI07-01G age model. Ages within the core range from 7.3 cal ka BP to 11.1 cal ka BP, with a mean error of ± 100 yrs. The age model was constructed using AMS $^{14}$C dating of marine molluc shells and benthic foraminifera. Ages were calibrated using the OxCal software version 4.2.4 (Ramsey, 2008) and the Marine13 curve (Reimer et al., 2013).

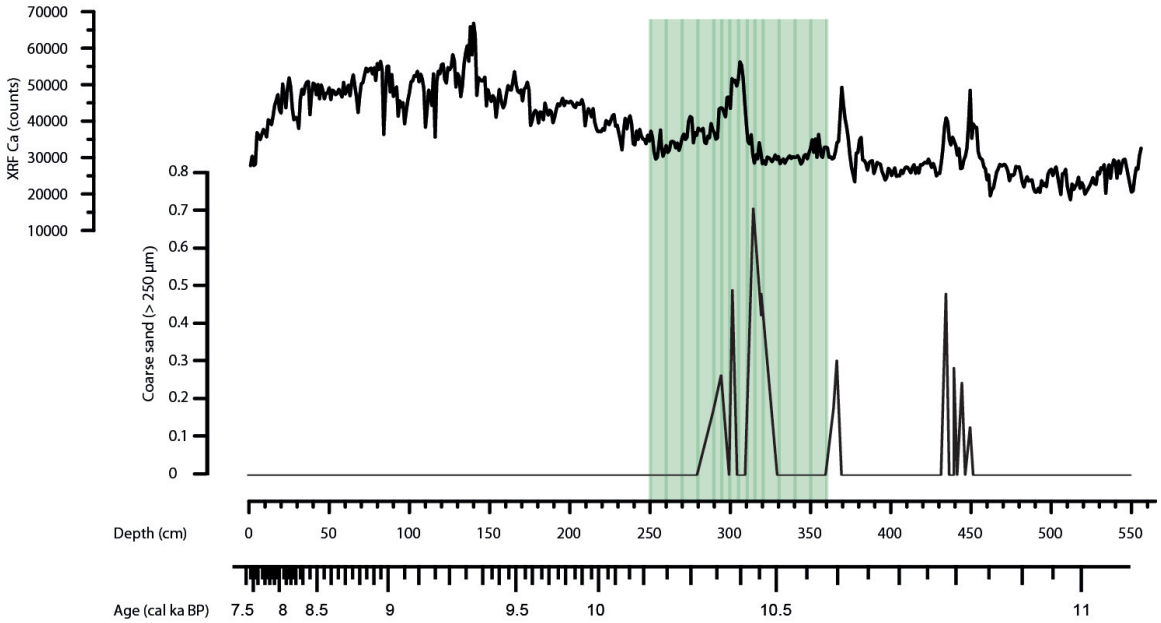


Figure 6: The coeval increase in coarse sand ($>$ 250 $\mu$m is displayed with the time series of XRF Ca counts. we observe three peaks in this coarse fraction during the period 10.3-11 cal ka BP

depths of 460; 430 and 370 cm. Again the peak centred around 307 cm is broad, but a large and rapid decrease in silt to the minima is observed coming out of the event ca. 280 cm. Following this, silt abundance increases to 82% throughout the remainder of the core, punctuated by broad, low amplitude peaks.

The sand fraction (both fine and coarse) overall shows an opposite trend to silt. Minima values correspond to peaks in silt. The appearance of coarse sand shows a remarkable correlation to the timing of Ca peaks throughout the core (Figure 6). Coarse sand appears at depths of 450, 370 and 310 cm and displays a range of between 0.1% and 0.8% of the total volume.

## 3.3 Geochemical analyses

XRF counts of Ca are stable throughout the older section of the core corresponding to 11.1-10.2 cal ka BP (550-255 cm), fluctuating around values ca. 30,000 counts (figure 7). This interval is punctuated by three peaks at 10.8, 10.6 and 10.4 cal ka BP (450, 370 and 307 cm). The peak corresponding to 307 cm sows a slower decline to peak values than the older peaks. The younger section of the core, from 10.2-7.4 cal ka BP (255-0 cm) shows a broad increase in Ca counts to the maxima of 65,000 at 9.2 cal ka BP (140 cm). Values fluctuate around 50,000 counts until 8 cal ka BP (30 cm) before rapidly plummeting back to values ca. 30,000 in the top 30 cm of the core.

There is very good correspondence between the XRF Ca counts and Ca/Sr throughout the core with the exception of a peak in Ca/Sr between 540-510 cm, with no contemporary peak in Ca and a slightly smaller peak at 140 cm. Values of Ca/Sr range between 8 and 24, fluctuating around 12 in the stable older section of the core. Likewise, this correlation is observed in calcium carbonate content ($CaCO_3$%) where values remain low (ca. 9%) during the older section of the core, before broadly rising and falling in synchronicity with Ca counts. Carbonate content varies between 6% and

17%, with a good distinction of the aforementioned peaks in Ca counts. The difference in sampling resolution between XRF proxies and $CaCO_3$ should be noted also.

The weight percentage of total organic carbon (TOC) shows a range between 0.1 % and 1.2 %. In general, TOC demonstrates a general decrease in the older section of the core from 11.1-10.4 cal ka BP (550-310 cm) from 0.8% to 0.4%. The trend reverses from 10.3 cal ka BP (280 cm) onwards throughout the core to reach the maximum value of 1.2%. With the exception of the peaks centred around 307 cm, the correlation of TOC and $CaCO_3$ is far more ambiguous than the aforementioned Ca-Ca/Sr relationship. Peaks observed in $CaCO_3$ do not always have a visible counterpart in TOC, and where they do, peak amplitudes vary greatly.

## 3.4 Diatoms

A total of 67 species from 21 genera were identified in core AI07-01G between 250-360 cm. The relative abundance of the most common species (those with concentrations over 3% in at least one sample) is shown in figure 8. Resting spores of *Chaetoceros* are abundant throughout the sampled interval, accounting for at least half of the diatom assemblage. As a result, resting spores are not shown and not counted towards the total number of diatoms. The absolute abundance of diatoms ranges from ca. 3 to 9 million valves per dry gram sediment. There appears to be a good agreement between absolute diatom abundance (ADA) and XRF Ca (counts). A considerable peak in ADA corresponds in depth with peaks in other proxies at a depth of ca. 307 cm. A second, broader peak of increased ADA is observed throughout 340-350 cm. However, the abundance of *Detonula confervacea* in these samples are particularly high, resulting in the diatom count of 300 being reached in a short surface area coverage, and thus potentially exaggerates this peak. Classifications of sea ice and cold water taxa used here are based on the scheme used by Weckström et al., (2013) applied to diatoms also from Bonavista Bay. There is a large increase in cold water taxa at 307 cm to their maximum abundance of 33 %. This is accompanied by a decrease in sea ice taxa minima at 305 cm. interestingly both taxa groups begin to deviate from background values at a depth of 320 cm. A second, smaller peak (and coincident trough) is observed in the cold water taxa at 295 cm.

*Detonula confervacea* resting spores are the most abundant species throughout the core, ranging from 24 to 60% of the total abundance. The abundance of *Detonula confervacea* increases at depths 350 (the maxima) and ca. 300. *Detonula confervacea* has been identified as an Arctic water species, being found in temperate North Atlantic waters during the winter months (Hasle, 1973). Both Hasle (1973) and Smayda (1969) observe that when present, *Detonula confervacea* are overwhelmingly dominant within the assemblage. *Fragilariopsis cylidrus* and *Fragilariopsis oceanica* are both Arctic water species associated with the presence of sea ice (Jensen et al., 2004). These species are present in large abundances throughout the core, however, neither species shows a particularly pronounced increase in abundance at any depth. With the exception of a very high value at 360 cm, *Fragilariopsis cylidrus* abundance fluctuates around 5% of the total abundance. Similarly the abundance of *Fragilariopsis oceanica* fluctuates around 10%.

*Thalassiosira nordenskioeldii* is a northern, cold water species often associated with spring blooms linked to melting sea-ice (Jiang et al., 2001). The abundance of *Thalassiosira nordenskioeldii* is very similar to *Fragilariopsis oceanica*, also peaking at 280 cm and decreasing in abundance at 300 cm. *Bacterosira bathyomphala* is a cold water species (Weckström et al., 2013; Krazcyk et al., 2012) whose abundance fluctuates around 3%. There is an increase between the depths 300-310 cm to ca. 6%. However, this is punctuated by a decrease (possibly as a result of dominance of *D. confervacea*). *Thalassiosira proschkinae* is a cosmopolitan species found as far north as 79 °N (Hasle and Thomas, 1997). This species exhibits slow decline in abundance from 340 to 307cm. followed by an abrupt increase to normal levels of ca. 6% at 295 cm.

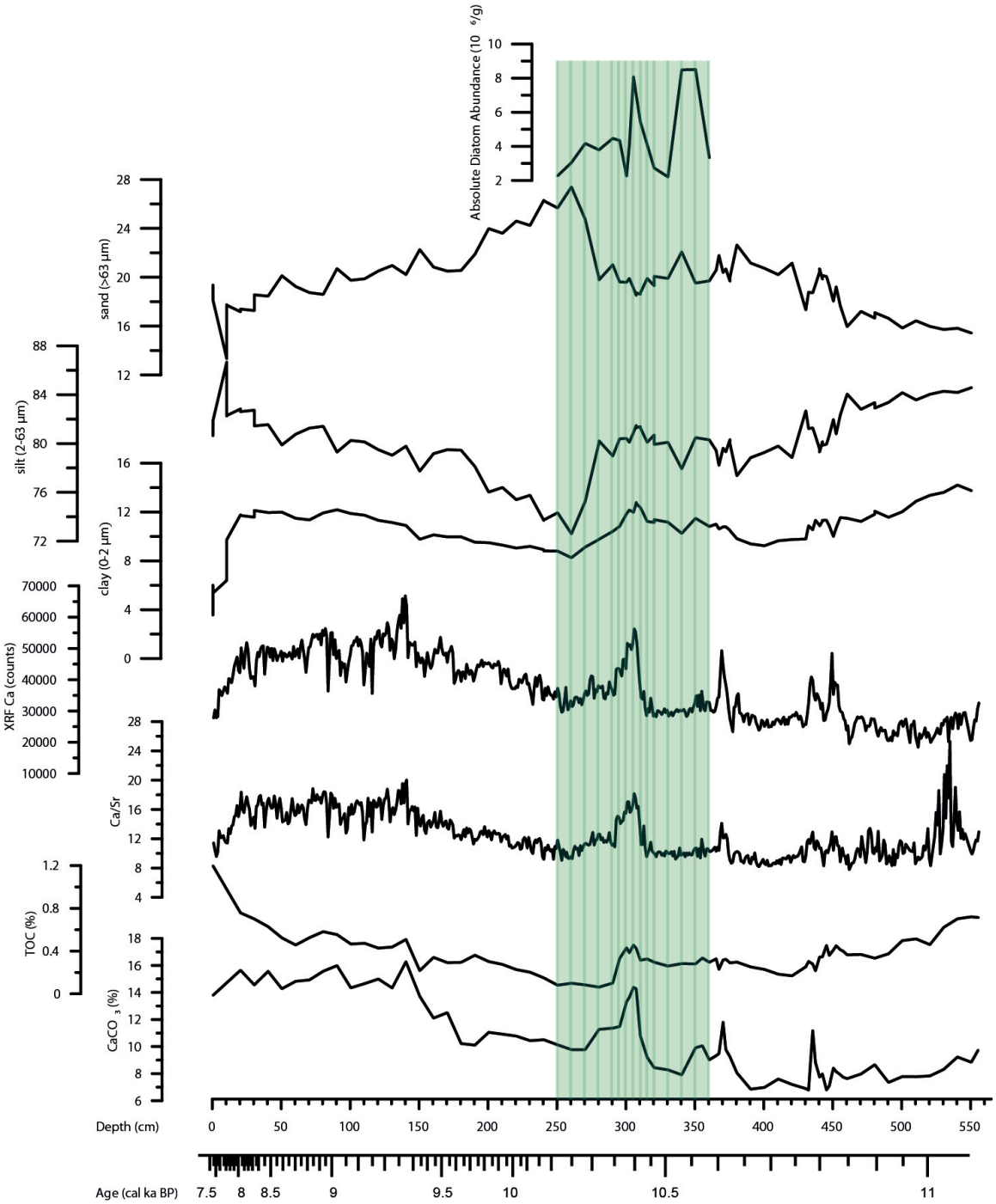


Figure 7: Results from geochemical and grain size analyses throughout core AI07-01G. The green box indicates the gold cove retreat, investigated using diatom assemblage counts. Dark green lines indicate the sample resolution throughout this period, except XRF which was sampled at 1 cm throughout the core.

*Thalassiosira hyalina* occurs in temperate to (sub)arctic waters and here demonstrate a decline into absence from 340 to 320 cm, followed by a gradual recovery back to values ca. 5% at 280 cm. *Thalassiosira gravida* and *Thalassiosira kushirensis*, both indicative of Arctic water assemblages and abundant in the Inner Labrador Current (De Sve, 1999; Weckstrm et al., 2014). Both species have low abundances (ca. 2%) except for a coeval increase from 295 to 320 cm. *Cocconeis costata* is a species tolerant of brackish water (Cremer, 1998). They are observed to have a fairly constant low abundance throughout. However, they are observed to be absent at depths 350 and 280 cm. *Navicula kariana*, and *Thalassiosira angulata* both have low abundances that do not show any pronounced peak or deviation from their means of 1 and 4% respectively.

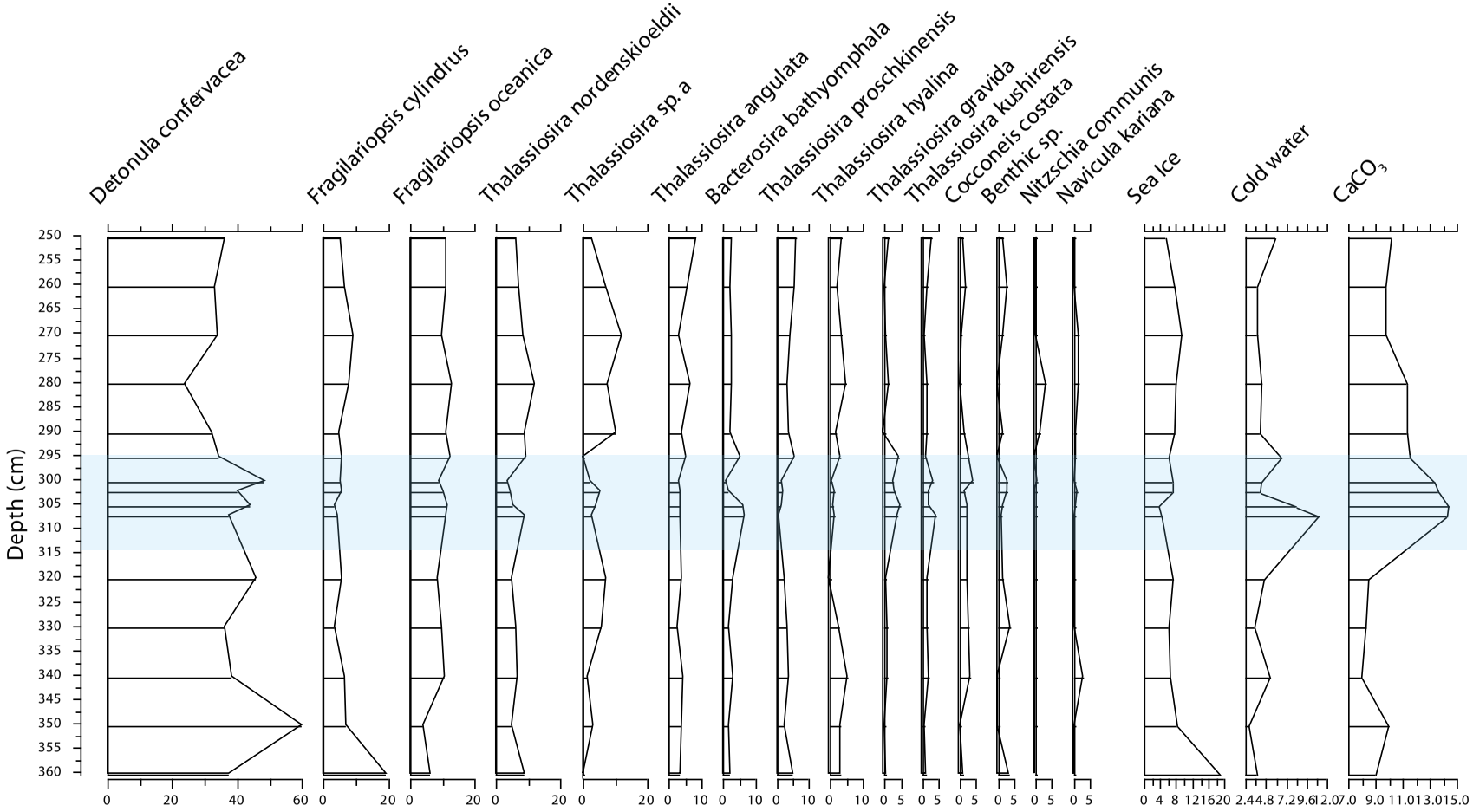


Figure 8: Diatom abundaces of species > 3%. We observe increased abundances of *B. bathyomphala*, *T. gravida* and *T. kushirensis* during the retreat of the glacial margin, highlighted here by the blue box. Classifcation of sea ice taxa and cold water species follows Weckström et al, (2013).

# 4 Discusion

## 4.1 Retreat of the Gold Cove glacial event

The well constrained age model of sediment core AI07−01G presented here, (FIGURE XX) places the timing of the Gold Cove retreat from 10,402-10,299 cal yrs BP ± 100 yrs. We propose that the retreat of the Laurentude glacial margin was not a discrete event, being known to last at least 200 radiocarbon years(Manley and Miller, 2001). As a reesult, an age range should be used when discussing the glacial retreat. Within this framework, we suggest that the peak rate of retreat occurred at 10,373 cal yrs BP, assuming that increased detrital carbonate input corresponds to increased melting and retreat (Andrews and Tedesco, 1992). Furthermore, based on the above assumption, the Gold Cove retreat can be described as having a short lived, rapid retreat phase, followed by a longer phase of slower retreat. The age range presented here agrees in timing with the Gold Cove retreat (DCP 2) presented by Jennings et al, (2015) at Cartwright Saddle, begining at 10,555 untill 10,405 cal ka. The slight differences in ages presented may be due uncertainties in the chronologies of both sediment cores.

One noticeable difference between the signatures of the Gold Cove retreat in both coves is the duration of the event, as evidenced by well constrained dates and detrital carbonate horizon thickness. Jennings et al, (2015) suggest that the glacial retreat lasted 150 years. However, we present data suggesting that at Bonavista Bay, increased carbonate sedimentation ,associated with the Gold Cove retreat, persisted for a shorter duration of 100 years. This is interesting in light of previously dated durations of ca. 200 radiocarbon years by Manley and Miller (2001). We propose two explanaitions for this apparant discrepancy in retreat duration between sites. Firstly, this may be a result of the subjective nature of choosing the start and end of the retreat by visual inspection of the data. This is also compliccated by resolution differences between the two sties, since at lower resolution, the event may appear to start earlier. Alternatively, we argue that the duration differences are a real feauture of a time transgressive deposit. In this scenario, during the early and final stages of glacial retreat, transport of detrital carbonate was limited to proximal regions on the labrador shelf. This could be due to less effiecient transport i.e. as a result of a weakened Labrador Current(Li et al., 2015), or reduced meltwater formation and calving. Thus, distal deposits may underestimate the full duration of teh glacial retreat considerably. As such, the thickest detrital layers (ca. 1 m thick at Sagalek Bank, Rashid et al., 2014) provide a better constraint of the full duration of the glacial retreat.

## 4.2 Transport of detrital carbonate during the Gold Cove retreat

We assume that the retreat phase of the Gold Cove glacial event was accompanied by large scale release of icebergs and freshwater both containing detrital carbonate, ground up from carbonate bedrock in the Hudson Strait source area (Andrews and Tedesco, 1992; Bond et al., 1992).

High Ca/Si ratios have been shown to distinguish detrital carbonate from carbonate of biogenic origin, due to the high proportion of Sr in biogenic Carbonate relative to chemically formed carbonate (Hodell and Curtis, 2008). Furthermore, Ca/Sr has been shown to be a powerful proxy when correlating detrital layers within the Labrador Sea (Channell et al., 2011). The remarkable correspondence exhibited between XRF Ca, $CaCO_3$ and Ca/Sr suggests that within Bonavista Bay, increased carbonate deposition during the early Holocene is a result of increased flux of detrital carbonate, not increased productivity. We observe that throughout the detrital carbonate layers, mean grain size increases considerably within the silt and clay (i.e. $<63$ $\mu$m) size range, suggesting that detrital carbonate is predominantly transported as fine sediment, rather than coarser material such as ice rafted debris (IRD) associated with iceberg calving.

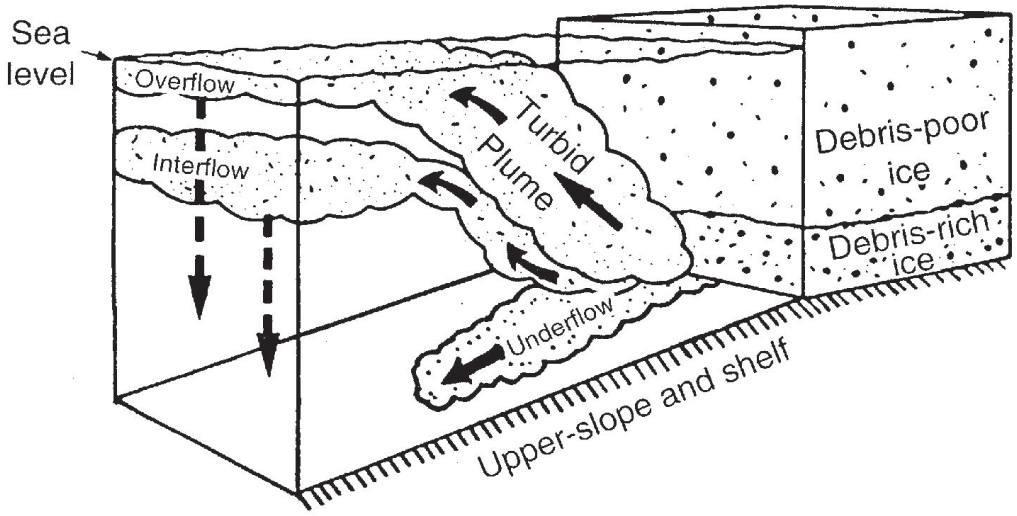


Figure 9: The formation of hyperpycnal plumes (underflow) and turbid plumes (glacial milk) by density differences between meltwater and ambient seawater. Turbid plumes rise and entrain fine clay and silt, transporting the material vast distances in suspension. Rashid et al, (2014) also propose deposition by a hyperpycnal plume at ice marginal localites. After Hesse et al, (1997).

Hesse et al, (1997) propose that due to desnity differences, in glacial meltwater and sediment is fractionated at its margin source. Glacial meltwater is of a lower density than the surrounding ambient sea water (figure 9). Thus, meltwater rises to the sea surface, entraining fine particles en route and creating a low density, clay silt rich freshwater plume at the surface, known as glacial milk (Hesse et al., 1997). In contrast, heavier grains (sand size particles) are deposited as bed load in the proximal region of melting. Suspended detrital carbonate, in the form of glacial milk, can be transported vast distances from source, because particle flocculation is greatly inhibited by carbonate presence, resulting in longer durations in suspension. As a result, turbid plume deposits have been found along the Labrador Shelf (Hesse at al., 1997). We suggest then that the vast majority of detrital carbonate input was transported as turbid fresh water plumes on this basis of increased silt and clay grain sizes. A similar scenario, invoking deposition by a hyperpycnal plume, has been proposed by Rashid et al, (2014) to explain the formation of coarse sand layers at Sagalek Bank.

Minor input of coarse sand is observed during the periods of peak Ca XRF counts. This corresponndence suggests that whilst the predominant mechanism of transport was as suspended load by turbidity plumes, some material was potentially transported by iceberg rafting processes. This coarse sand fraction would not be able to remian in suspension over such vast distances. Increased ice rafted debris (IRD, grain size >2 mm) observed at Cartwright Saddle (Jennings et al., 2015) during the Gold Cove retreat also suggest that transport and deposition at localities north of Newfoundland was influenced, albeit to a greater extent, by icebergs. As such, we argue that icebergs calved from the east margi of the Laurentide ice sheet and were transported south along the Labrador Shelf in a freshwater plume 'soup'. However, upon reaching Cartwright Saddle, icebergs carrying coarse material potentially tracked east, confined to the deeper waters of the shelf margin and Outer Labrador Current (Rashid et al., 2011). Alternatively, icebergs mmay have continued south along

the Labrador Shelf, transported by the Inner Labrador Current, but potentially melted and reduced in volume and thus deposition, between Cartwright Saddle and Newfoundland.

Hill and Condron (2014) have modelled the propagation pathway of meltwater in the Labrador Sea. They observe that low salinity water travels along the Labrador coast as a narrow coastal boundary current, before turning south at the Flemish Cap and reaching the subtropical Atlantic region. This results in little penetration of the surface water into the inner Labrador sea and North Atlantic. Perhaps the icebergs tracked east whilst turbid plumes continued south to Newfoundland. Jennings et al, (2015) provide a record of decreasing sea surface salinity using $\delta^{18}$O from the planktonic foraminifera species *G. bulloides*. However, the diatom assemblage at Bonavista Bay show no considerable increase in sea ice taxa or brackish species. This may be a function of proxy sensitivity, Weckström et al, (2014) suggests that IP25 may record changes in sea better than diatom assemblages for example. As such it is difficult to constrain if icebergs did indeed pass by Bonavista Bay. This is further complicated by the fact that Bonavista Bay is annualy covered by sea ice and sample resolution exceeds one year.

Detritus in modern icebergs is principally composed of sand sized particles (>63$\mu$m). However, Hesse and Khodabakhsh (1998) argue that as a result of more efficient bedrock grinding under thicker ice sheets, Laurentide source icebergs may have transported a considerably higher amount of silt and clay. If this is indeed the case, it complicates our interpretation of deposition by a turbid plume because of the intrinsic difficulty in differentiating between detrital carbonate from a plume and from a melting iceberg.

## 4.3 Increased strength of the Labrador Current during the Gold Cove Event and increased Arctic input

Whilst no systematic increase in sea ice taxa is observed, a broad peak in cold water species, as well as the appearance of Arctic species accompany the Gold Cove retreat. The diatom species *Thalassiosira gravida* has been recognised as a cold water species, strongly associated with Arctic assemblages and indicative of surface temperatures between 1.5-2 °C and low salinities between 27-31‰ (Scott and Collins, 1996; De Seve, 1999). Whilst there is considerable debate surrounding the taxonomy of, and vegetative spore responsible for the formation of *Thalassiosira kushirensis*((*T. gravida* or *T. Antarctica* var. Borealis), Weckström et al, (2014) point out that *T. Kushirensis* it is still indicative of cold Arctic water assemblages. The coeval increase in abundance of both *T. gravida* and *T. kushirensis* presented here (Figure XX) supports the argument that *T. kushirensis* is a resting spore of the vegetative *T. gravida* (De Seve, 1996; Pearce et al., 2014). Clearly, more detailed investigation into the taxonomy of this group of species is required to resolve this issue, however, we follow the tradional ecological classification of this species as an indicator of Arctic water. Furthermore, *T. gravida* spores (*T. kushirensis*) have been shown to dominate assemblages further north in the Baffin Bay region (De Seve, 1996).

Here, increased abundances of diatom species *Thalassiosira kushirensis* and *Thalassiosira gravida* during the gold cove retreat is considered indicative of a greater Arctic water influence and, and stronger Inner Labrador Current in core AI07-O1G during the gold cove retreat is considered as indicative of a greater influence of Arctic water within the Inner Labrador Current. The increased flux of meltwater to the Labrador Sea potentially results in the strengthening of the Labrador Current(Scott and Collins, 1996; Rashid et al., 2011; Li et al., 2015). This has been found to be the predominant control on Labrador Current strength over geological time scales (Li et al., 2015). Whilst the melting of the Laurentide ice sheet was likely caused by increased temperatures on land, the increased influence of Arctic waters possibly kept the sea surface temperatures cold (Scott and Collins, 1996). This is supported by the increase in cold water taxa, particulary *Bacterosira*

*bathyomphala* and a lack of warm/temperate species (*Thalassionema nitzschioides*, *Rhizosolenia sp.*, *Thalassiosira. oestrupi*) throughout the Gold Cove retreat. The apparent strengthening of the Labrador Current may have resulted in the cooling of temperatures over land (Scot and Collins, 1996) and caused the ending of the Gold ove Event. Furthermore, increased strength of the Inner Labrador Current would result in the further transport of the aforementioned turbid plume (Hesse et al., 1997).

## 4.4 The biogenic repsonse to glacial retreat

The observed increase in TOC (wt.%) and absolute diatom abundace (ADA) throughout the Gold Cove retreat, suggests that primary productivity is greatly affected during glacial retreat. However, these data disgaree with previously modelled studies of North Atlantic productivity response to Heinrich events (Sachs et al., 2005; Nave et al., 2007; Mariotti et al., 2012). As such, it is most likely that the increased productivity observed at Bonavista Bay is a result of local upwelling. However, it is not known if the source of nutrients is meltwater from Hudson Strait, or a more local source. Hudson Bay has been suggested as a source of nutrients to the labbrador shelf by (Sutcliffe et al., 1983). If indeed the source region is related to Hudson Strait, then an increase in productivity across the Labrador Shelf at localities north of Newfoundland is expected.

## 4.5 Implications

Our findings suggest that the east margin of the Laurentide ice sheet was characterised by a number of different processes during the retreat of its margin. The timing of freshwater flux to the North Atlantic suggests that the Gold Cove event may have perturbed oceanic circulation, resulting in a trans-atlantic tele connection, and subsequent climate cooling in Europe (Broecker, 1994). Whilst icebergs may have entered the North Atlantic region directly, it is important to consider the effect of freshwater plumes which are capable of travelling vast distances and contributing to the slowing down of ocean overturning (Hill and Condron, 2014).

## 4.6 Limitations

### 4.6.1 Chronology

Whilst a marine reservoir offset ($\Delta$R) of 50 $\pm$ 50 years was selected to correlate our event to events presented by Jennings et al, (2015), it should be noted that due to considerable uncertainty in the extent and duration of Labrador sea ice cover, which prevents carbon exchange between the ocean-atmospher, during the early Holocene, there is a large uncertainty in this age range (Jennings et al., 2015). $\Delta$R values used in previous studies range from 50  1,000 years, with most values set at ca. 350 years (Lewis et al., 2012; Rashid et al., 2014; Jennings et al., 2015). Unfortunately given that there are no absolute dated horizons, such as tephra layers, the issue of how large of a local marine reservoir offset to use is still a largely undetermined factor.

However, regardless of absoolute age values, we are able to present a well constrained radiocarbon age ($^{14}$C ka BP) which can be used to correlate core AI07-O1G to other records throughout the Labrador Shelf region when a common reservoir offset is applied. Thus, whilst uncertainites in the absolute age (cal ka BP) are potentially very large, we suggest that the correlative potential is very robust.

### 4.6.2 Diatoms

An important consideration when interpreting micropaleontological data, is the extent to which the fossil record is representative of the living assemblage it represents. Dissolution is by far the greatest control on the integrity of the fossil record. In general, the ocean is under-saturated with respect to silica, resulting in dissolution of the frustrule at the sediment surface and within the top few centimetres of the sea-floor. The result of this dissolution is the removal of lightly silicified diatoms (*Chaeteceros* vegetative cells) and a bias towards heavily silicified species and resting spores (Mikkelsen, 1977). Nelson et al, (1995) suggest that up to 50% of biogenic silica is lost to dissolution in the top 100 m of the water column, and subsequently a loss of 95% of the living flora before reaching the sea floor (Nelson et al., 1995). The flora presented herein is heavily dominated by resting spores of *Chaeteceros* and *Detonula confervacea*. Whilst the assumption in the interpretation of these data has been that the fossil record is representative of the living flora, it should be noted that dissolution of less silicified diatom could have potentially occurred.

Mechanical processes, such as winnowing and physical break up of diatoms also leads to fossil record bias. Breakdown of larger diatoms, such as *Coscinodiscus* and *Actinocyclus* also results in the loss of environmental data because they cannot be identified or counted. In the light of this, it is not fully appreciated if the mechanical breakdown of diatoms in core AI07-01G results from methodological procedures, or diagenesis. However, during assemblage counts, diatoms as small as 5 $\mu$m were observed. Thus, it would appear that winnowing has not been a major factor at this site during the interval investigated.

The taxonomy and ecological interpretation of species, upon which paleoceanographic interpretations are based, is inevitably subjective. The misidentification of species between authors has led to a plethora of synonyms within the taxonomic literature, and debate as to the ecological habitat of the species (see Weckstrm et al., 2014 and Krawczyk et al., 2012 for example). Whilst misidentification can never be totally ruled out, utmost care has been taken to ensure correct identification to species, and the taxonomy literature used has been reported in detail in the methods description.

### 4.6.3 Grain size analyses

The main assumption of the grain size analysis is that the small sample used is homogeneous and representative of the overall lithology. However, given the small amount of IRD present by Jennings et al, (2015), by using only a small sample, important IRD grains may be missed within the sample. Possible methods to overcome this may be to sieve the samples through a series of different fraction sieves, or alternatively to perform and x-radiograph of the core and count the grains visible (Jennings et al., 2015).

Another consideration of the analysis is the absence of an acid pre-treatment to remove carbonate as in Jennings et al, (2015). Since we are investigating detrital carbonate deposites, then acid-treatment would result in considerable loss of data and leave only siliceous material. A more robust method would be to analyse grain size both with and without carbonate, to better constrain the changing grain size through these detrital carbonate events.

## 4.7 Future work

We suggest that future research investigate the changes in salinity in Bonavista Bay, using benthic $\delta^{18}$O stable isotopes, as due to the shallow water depth, the signal should be similair should be similair to that of planktonic species. Proxies of sea ice (IP25) should also be innvestigated in order to ascertain the extent of increased sea ice in the form of icebergs in the area. Changes in productivity during the retreat should be investiggated at proximal localities on the labrador shelf.

Furthermore, diatom assemblages during the detrital carbonate peaks possibly corresponding to the Noble Inlet Advance and the Younger Dryas (H0) events should be investigated to ascertain if the strengthening of the Labrador Current is a unique feature of the Gold Cold event, or common to all of the recorded glacial advances.

# 5 Conclusions

A multi-proxy approach was used to reconstruct the nature and timing of a detrital carbonate layer, associated with a local readvance of the east margin of the Laurentide Ice Sheet over the Hudson Strait and Frobisher Bay. We find that;

(i) based on radiocarbon dating of mollusc shells and benthic foraminifera samples, the age of the Gold Cove retreat in core AI07-01G (as recorded by carbonate detritus) begins at 10.4 cal ka BP and ends 10.3 cal ka BP ± 100 yrs. We suggest that peak melting occurred ca. 10,370 cal yrs BP, corresponding to peak XRF Ca counts. These ages agree with previously published ages of the Gold Cove retreat from the Labrador Shelf. We acknowledge that whilst the age of the Gold Cove retreat in Bonavista Bay is well constrained by a high number of radiocarbon dates, the robustness of this age range is unknown due to large uncertainties in $\Delta$R of the Labrador Sea during the early Holocene;

(ii) transport of detrital carbonate to Bonavista Bay was predominantly in the form of fresh water turbidity plumes carrying silt. However, very small percentages of course sand suggests a decreasing influence of icebergs passing past the bay and transporting coarser material (i.e. > 2mm IRD) this far south of the Hudson Strait. This is possibly due to the re-routing of icebergs, prior to reaching Newfoundland, to deeper water along the shelf margin. . Alternatively, increased air temperatures may have resulted in melting of icebergs between Cartwright Saddle and Bonavista Bay and as such reduced influence. It should be noted that due to uncertainties in the grain size transported by paleo-icebergs, this is very difficult to constrain;

(iii) increased flux of freshwater to the Labrador Sea during the Gold Cove retreat resulted in the strengthening of the Inner Labrador Current and greater influence of cold Arctic Water, and consequently cold surface temperature. This is supported by increased abundances of diatom species indicative of Arctic Assemblages i.e. *Thalassiosira gravida*, *Thalassiosira kushirensis* and the cold water species *Bathyomphala bacterosira*;

(iv) increased flux of meltwater to Bonavista Bay resulted in increased diatom productivity. However, it as yet unknown if this is due to the advection of nutrients from Hudson Strait along the Labrador shelf, or more local isolated upwelling induced by the Gold Cove retreat.

In summary, we propose that the Gold Gove Event occurred 10.4 cal ka BP ± 100 years. The event was characterised by the release of detrital carbonate in the form of turbid plumes, hyperpycnal plumes and possibly icebergs from the eastern margin of the LIS. Increased meltwater flux resulted in the strengthening of the Inner Labrador Current and increased Arctic Water influence. The increased strength of the ILC resulted in colder sea surface waters, and reduced temperatures on land, possibly resulting in the cessation of the meltwater event. Furthermore, it is likely that the detrital carbonate plume tracked southwards past Newfoundland and toward the subtropics before perturbing the AMOC and consequently circum Atlantic climate. As a result, the best records for correlating detrital carbonate peaks are expected to be found on the Labrador Shelf, as different processes operate seaward of Hudson Strait.

## Acknowledgments

Christof Pearce is thanked for supervision, guidance and constructive discussion throughout the project. Marit-Solveig Seidenkrantz is thanked for assistance in foraminifera and mollusc taxonomy, and Nicolas Van Nieuwenhove for assistance in sampling, both at Aarhus University. Jesper Olsen and the $^{14}$C AMS dating laboratory at Aarhus University are also thanked for prompt dating of samples. Christian Stranne is acknowledged for providing new insights in the grain size data. Carina Johansson is thanked for laboratory assistance at Stockholm University.

The Department of Geological Sciences at Stockholm University (particularly Rienk Smittenberg and Elisabeth Däcker) are thanked for facilitating the academic exchange and for administrative duties prior to and during the stay.

# References


Aksenov, Y., Bacon, S., Coward, A. C., and Holliday, N. P. (2010). Polar outflow from the Arctic Ocean: A high resolution model study. *Journal of Marine Systems*, 83(1-2):14–37.

Andersen, C., Koç, N., and Moros, M. (2004). A highly unstable Holocene climate in the subpolar North Atlantic: Evidence from diatoms. *Quaternary Science Reviews*, 23(20-22 SPEC. ISS.): 2155–2166.

Andrews, J. T. and MacLean, B. (2003). Hudson Strait ice streams: A review of stratigraphy, chronology and links with North Atlantic Heinrich events. *Boreas*, 32(1):4–17.

Andrews, J. T. and Tedesco, K. (1992). Detrital carbonate-rich sediments, northwestern Labrador Sea: implications for ice-sheet dynamics and iceberg rafting (Heinrich) events in the North Atlantic. *Geology*, 20(12):1087–1090.

Andrews, J. T., Jennings, A. E., Kerwin, M. W., Kirby, M. E., Manley, W., Miller, G., Bond, G., and Maclean, B. (1995). A Heinrich-like event, H-0 (DC-0): source(s) for detrital carbonate in the North Atlantic during the Younger Dryas chronozone. *Paleoceanography*, 10(5):943–952.

Andrews, J. T., Keigwin, L., Hall, F., and Jennings, A. E. (1999). Abrupt deglaciation events and Holocene palaeoceanography from high-resolution cores, Cartwright Saddle, Labrador Shelf, Canada. *Journal of Quaternary Science*, 14(5):383–397.

Barber, D. C., Dyke, A., Hillaire-Marcel, C., Jennings, A. E., Andrews, J. T., Kerwin, M. W., Bilodeau, B., McNeely, R., Southon, J., Morehead, M. D., and Gagnon, J.-M. (1999). Forcing of the cold event of 8,200 years ago by catastrophic drainage of Laurentide lakes. *Nature*, 400((4)): 344–348.

Bérard-Therriault, L., Poulin, M., and Bossé, L. *Guide didentification du phytoplancton marin de lestuaire et du golfe du Saint-Laurent: incluant également certains proto- zoaires.* NRC Research Press, Ottawa.

Bond, G., Heinrich, H., Broecker, W., Labeyrie, L., McManus, J., Andrews, J., Huon, S., Jantschik, R., Clasen, S., Simet, C., Tedesco, K., Klas, M., Bonani, G., and Ivy, S. (1992). Evidence for massive discharges of icebergs into the North Atlantic ocean during the last glacial period. 360 (6401):245–249.

Broecker, W. S. (1994). Massive iceberg discharges as triggers for global climate change. *Nature*, 372(6505):421–424.

Canadian Ice Service. (2013). Climatic Ice Atlas 1981 2010. pages http://www.ec.gc.ca/glaces–ice.

Channell, J. E. T., Hodell, D. A., Romero, O., Hillaire-Marcel, C., de Vernal, A., Stoner, J. S., Mazaud, A., and Röhl, U. (2012). A 750-kyr detrital-layer stratigraphy for the North Atlantic (IODP Sites U1302-U1303, Orphan Knoll, Labrador Sea). *Earth and Planetary Science Letters*, 317-318:218–230.

Clark, C. D., Knight, J. K., and Gray, J. T. (2000). Geomorhological reconstruction of the Labrador Sector of the laurentide ice Sheet. *Quaternary Science Reviews*, 19:1343–1366.

Cremer, H., (1998). *The diatom flora of the Laptev Sea (Arctic Ocean).* J, Cramer, Berlin and Stuttgart.

Cumming, E. H., Aksu, A. E., and Mudie, P. J. (1991). Late Quaternary glacial and sedimentary history of Bonnavista Bay, northeast Newfoundland. *Canadian Journal of Earth Sciencesa*, (29): 222–235.

De Sève, M. A. (1999). Transfer function between surface sediment diatom assemblages and sea-surface temperature and salinity of the Labrador Sea. *Marine Micropaleontology*, 36:249–267.

Deser, C., Holland, M., Reverdin, G., and Timlin, M. (2002). Decadal variations in Labrador Sea ice cover and North Atlantic sea surface temperatures. *Journal of Geophysical Research-Oceans*, 107:3–1–3–12.

Drinkwater, K. F. (1996). Atmospheric and oceanic variability in the northwest Atlantic during the 1980s and early 1990s. *Journal of Northwest Atlantic Fishery Science*, 18:77–97.

Fairbanks, R. G. (1989). A 17,000-year glacio-eustatic sea level record: influence of glacial melting rates on the Younger Dryas event and deep-ocean circulation. 342(6250):637–642.

Fratantoni, P. and McCarrtney, M. (2010). Freshwater export from the Labrador Current to the North Atlantic Current at the Tail of the Grand Banks of Newfoundland. *Deep Sea Research Part 1: Oceanographic Reasearch Papers*, 57(2):258–283.

Gersonde, R., Crosta, X., Abelmannn, A., and Armand, L. (2005). Sea surface temperature and sea ice distribution of the last glacial Southern - A circum-Antarctic view based on siliceous microfossil records. *Quaternary Science Reviews*, 24(7-9):869–896.

Hasle, G. (1973). Some marine plankton genera of the diatom family Thalassiosiracae. *Beiheft zur Nova Hedwigia*, (45):1–68.

Hasle, G. and Syvertsen, E. Marine diatoms. In Tomas, C., editor, *Identifying marine phytoplankton*, pages 5–385. Academic Press, California, (1997).

Hemming, S. R. (2004). Heinrich events: Massive late Pleistocene ditritus layers of the North Atlanitc and their global cliamate imprint. *Review of Geophysics*, 42(2003):RG1005 doi:10.1029/2003RG000128.

Hesse, R. and Khodabakhsh, S. (1998). Depositional facies of late Pleistocene Heinrich events in the Labrador Sea. *Geology*, 26(2):103–106.

Hesse, R., Khodabakhsh, S., Klaucke, I., and Ryan, W. B. F. (1997). Asymmetrical turbid surface-plume deposition near ice-outlets of the Pleistocene Laurentide ice sheet in the Labrador Sea. *Geo-Marine Letters*, 17(3):179–187.

Hill, J. C. and Condron, A. (2014). Subtropical iceberg scours and meltwater routing in the deglacial western North Atlantic. *Nature Geoscience*, 7(11):806–810.

Hillaire-Marcel, C., de Vernal, A., Bilodeau, G., and Wu, G. (1994). Isotope stratigraphy, sedimentation rates, deep circulation, and carbonate events in the Labrador Sea during the last ˜200ka. 31(1):63–89.

Hodell, D. a. and Curtis, J. H. (2008). Oxygen and carbon isotopes of detrital carbonate in North Atlantic Heinrich Events. *Marine Geology*, 256(1-4):30–35.

Jennings, A., Andrews, J., Pearce, C., Wilson, L., and Ólfasdótttir, S. d. (2015). Detrital carbonate peaks on the Labrador shelf, a 137ka template for freshwater forcing from the Hudson Strait outlet of the Laurentide Ice Sheet into the subpolar gyre. *Quaternary Science Reviews*, 107:62–80.

Jensen, K. G., Kuijpers, A., Koç, N., and Heinemeier, J. (2004). Diatom evidence of hydrographic changes and ice conditions in Igaliku Fjord, South Greenland, during the past 1500 years. 14(2): 152–164.

Johnsen, S. J., Clausen, H. B., Dansgaard, W., Fuhrer, K., Gundestrup, N., Hammer, C. U., Iversen, P., Jouzel, J., Stauffer, B., and Steffensen, J. P. (1992). Irregular glacial interstadials recorded in a new Greenland ice core. 359(6393):311–313.

Julius, M. L. and Theriot, E. C. The diatoms: a primer. In Smol, J. P. and Stoermer, E. F., editors, *The diatoms: Applictaions for the environmental and Earth Sciences*, chapter 2, pages 8–22. Cambridge University Press, Cambridge, 2 edition, (2010).

Karpuz, N. K. and Jansen, E. (1992). A high-resolution diatom record of the last deglaciation from the SE Norwegian Sea: Documentation of rapid climatic changes. 7(4):499.

Kaufman, D. S., Miller, G. H., Stravers, J. A., and Andrews, J. T. (1993). Abrupt early Holocene (9.9–9.6 ka) ice-stream advance at the mouth of the Hudson Strait, Arctic Canada. *Geology*, 21: 1063–1066.

Kirby, M. E. and Andrews, J. (1999). Mid-Wisconsin Laurentide ice sheet growth and decay: Implications for Heinrich events 3 and 4. *Paleoceanography1*, 14(2):211–223.

Krawczyk, D. W., Witkowski, A., Wroniecki, M., Waniek, J., Kurzydowski, K. J., and Pociski, T. (2012). Reinterpretation of two diatom species from the West Greenland margin - Thalassiosira kushirensis and Thalassiosira antarctica var. borealis - hydrological consequences. *Marine Micropaleontology*, 88-89:1–14.

Lazier, J. R. N. and Wright, D. G. (1993). Annual Velocity Variations in the Labrador Current. 23 (4):659–678.

Leventer, A., Crosta, X., and Pike, J. Holocene marine diatom records of environmental change. In Smol, J. P. and Stoermer, E., editors, *The diatoms: Applictaions for the environmental and Earth Sciences*, chapter 21, pages 401–423. Cambridge University Press, Cambridge, 2 edition, (2010).

Lewis, C. F. M., Miller, A. A. L., Levac, E., Piper, D. J. W., and Sonnichsen, G. V. (2012). Lake Agassiz outburst age and routing by Labrador Current and the 8.2 cal ka cold event. *Quaternary International*, 260:83–97.

Li, G. and Piper, D. J. (2015). The influence of meltwater on the Labrador Current in Heinrich event 1 and the Younger Dryas. *Quaternary Science Reviews*, 107:129–137.

MacAyeal, D. R. (1993). Binge/purge oscillations of the Laurentide Ice Sheet as a cause of the North Atlantic's Heinrich events. *Paleoceanography*, 8(6):775–784.

Manley, W. and Miller, G. Glacial-geological record on southern Baffin Island reflecting late glacial ice-sheet dynamics in the eastern Hudson Strait region. In Maclean, B., editor, *Marine Geology of Hudson Strait and Ungava Bay, Eastern Arctic Canada; Late Quaternary Sediments, Depositional Environments, and Late Glacial-Deglacial History Derived from Marine and Terrestrial Studies*, pages 19–30. Queens Printer, Ottawa, geological edition, (2001).

Mertz, G., Narayanan, S., and Helbig, J. (1993). The freshwater transport of the Labrador Current. *Atmosphere-Ocean*, 31:281–295.

Mikkelsen, N. (1977). Silica dissolution and overgrowth of fossil diatoms. *Micropaleontology*, (23): 223–6.

Miller, G. H. and Kaufman, D. S. (1990). Rapid fluctuations of the Laurentide ice sheet at the mouth of Hudson Strait: New evidence for ocean/ice-sheet innteractions as a control on the Younger Dryas. *North*, 5(6):907–919.

Miller, K. R. and Chapman, M. R. (2013). Holocene climate variability reflected in diatom-derived sea surface temperature records from the subpolar North Atlantic. *The Holocene*, 23(6):882–887.

Mortyn, P. G. and Charles, C. D. (2003). Planktonic foraminiferal depth habitiat an d18O calibrations: Plankton tow results from the Atlantic sector of the Southern Ocean. *Paleoceanography*, 18 (2):doi:10.1029/2001PA000637.

Nave, S., Labeyrie, L., Gherardi, J., Caillon, N., Cortijo, E., Kissel, C., and Abrantes, F. (2007). Primary productivity response to Heinrich events in the North Atlantic Ocean and Norwegian Sea. *Paleoceanography*, 22(3):1–18.

Nelson, D. M., Tr eguer, P., Brzezinski, M. A., Leynaert, A., and Qu eguiner, B. (1995). Production and dissolution of biogenic silica in the ocean: revised global estimates, comparison with regional data and relationship to biogenic sedimentation. *Global Biogeochemical Cycles*, (9):359–372.

Pearce, C. (2015). The timing of the Gold Cove glacial event: A comment on Signature of the Gold Cove event (10.2 ka) in the Labrador Sea. *Quaternary International*, page http://dx.doi.org/10.1016/j.quaint.2015.02.67.

Pearce, C., Seidenkrantz, M.-S., Kuijpers, A., and Reynisson, N. F. (2014)a. A multi-proxy reconstruction of oceanographic conditions around the Younger DryasHolocene transition in Placentia Bay, Newfoundland. *Marine Micropaleontology*, 112:39–49.

Pearce, C., Weckström, K., Sha, L., Miettinen, A., and Seidenkrantz, M.-S. (2014)b. The Holocene marine diatom flora of Eastern Newfoundland bays. *Diatom Research*, 29(4):441–454.

Petrie, B. (2007). Does the north Atlantic oscillation affect hydrographic properties on the Canadian Atlantic continental shelf? 45(3):141–151.

Petrie, B. and Anderson, C. (1983). Circulation on the newfoundland continental shelf. *Atmosphere-Ocean*, 21(2):207–226.

Prater, M. D. (2002). Eddies in the Labrador Sea as Observed by Profiling RAFOS Floats and Remote Sensing. 32(2):411–427.

Prinsenberg, S., Peterson, I., Narayanan, S., and Umoh, J. (1997). Interaction between atmosphere, ice cover, and ocean off Labrador and Newfoundland from 1962 to 1992. *Canadian Journal of Fisheries and Aquatic Sciences*, 54:30–39.

Rahmstorf, S. (1995). Bifurcations of the Atlantic thermohaline circulation in response to changes in the hydrological cycle. 378(6553):145–149.

Ramsey, C. B. (2008). Deposition models for chronological records. *Quaternary Science Reviews*, 27(1-2):42–60.

Rashid, H., Piper, D. J. W., and Flower, B. P. (2011). The role of Hudson Strait outlet in younger dryas sedimentation in the Labrador Sea. *Geophysical Monograph Series*, 193(1):93–110.

Rashid, H., Piper, D. J., Mansfield, C., Saint-Ange, F., and Polyak, L. (2014). Signature of the Gold Cove event (10.2 ka) in the Labrador Sea. *Quaternary International*, 352:212–221.

Reimer, P., Bard, E., Bayliss, A., Beck, J., Blackwell, P., Ramsey, C., Buck, C., Cheng, H., Edwards, R., Firedrich, M., Grootes, P., Guilderson, T., Haflidason, H., Hajdas, I., Hatte, C., Heaton, T., Hoffmann, D., Hogg, A., Hughen, K., Kaiser, K., Kromer, B., Manning, S., Niu, M., Reimer, R., Richards, D., Scott, E., Southon, J., Staff, R., Turney, C., and Plicht, J. (2013). IntCal13 and Marine13 Radiocarbon Age Calibration Curves 050,000 Years cal BP. *Radiocarbon*, 55(4): 1869–1887.

Sachs, J. P. and Anderson, R. F. (2005). Increased productivity in the subantarctic ocean during Heinrich events. *Nature*, 434(7037):1118–1121.

Scott, D. B. and Collins, E. S. (1996). Late mid-holocene sea-level oscillation: A possible cause. *Quaternary Science Reviews*, 15(8-9):851–856.

Smayda, T. J. (1969). Experimental observations on the influence of temperature, light, and salinity on cell division of the marine diatom, Detonula confervacea (Cleve) Gran. *Journal of Phycology*, 5:150–157.

Solignac, S., Seidenkrantz, M.-S., Jessen, C., Kuijpers, a., Gunvald, a. K., and Olsen, J. (2011). Late-Holocene sea-surface conditions offshore Newfoundland based on dinoflagellate cysts. *The Holocene*, 21(4):539–552.

Sutcliffe, W. H., Loucks, R. H., Drinkwater, K. F., and Coote, A. R. (1983). Nutrient flex onto the Labrador Shelf from Hudson Strait and its Biological Consequences. *Canadian Journal of Fisheries and Aquatic Sciences1*, 40(10):1692–1701.

Törnqvist, T. E. and Hijma, M. P. (2012). Links between early Holocene ice-sheet decay, sea-level rise and abrupt climate change. *Nature Geoscience*, 5(9):601–606.

Veillette, J., a.S. Dyke, and Roy, M. (1999). Ice-flow evolution of the Labrador Sector of the Laurentide Ice Sheet: a review, with new evidence from northern Quebec. *Quaternary Science Reviews*, 18(8-9):993–1019.

Warnock, J. P. and Scherer, R. P. (2014). A revised method for determining the absolute abundance of diatoms. *Journal of Paleolimnology*, 53(1):157–163.

Weckström, K., Massé, G., Collins, L. G., Hanhijärvi, S., Bouloubassi, I., Sicre, M. A., Seidenkrantz, M. S., Schmidt, S., Andersen, T. r. J., Andersen, M. L., Hill, B., and Kuijpers, A. (2013). Evaluation of the sea ice proxy IP25 against observational and diatom proxy data in the SW Labrador Sea. *Quaternary Science Reviews*, 79:53–62.

Weckström, K., Miettinen, A., Caissie, B., Pearce, C., Ellegaard, M., Krawczyk, D., and Witkowski, A. (2014). Sea surface temperatures in Disko Bay during the Little Ice Age - caution needs to be exercised before assigning Thalassiosira kushirensis resting spore as a warm-water indicator in palaeoceanographic studies. *Quaternary Science Reviews*, 101:234–237.

Wiersma, A. P. and Jongma, J. I. (2010). A role for icebergs in the 8.2 ka climate event. *Climate Dynamics*, 35(2):535–549.

Witkowski, A., Lange-Bertalot, D., and Metzeltin, H., (2000). *Diatom flora of marine coasts*. A.R.G. Gantner, Ruggell.

# Apendices

## Appendix A

### Grain size data

| Age (cal yrs BP) | Mid-point depth (cm) | 0 - 2 $\mu$m | 2 - 10 $\mu$m | 10 - 63 $\mu$m | 63 - 2500$\mu$m |
|---|---|---|---|---|---|
| 7356.6 | 0.5 | 3.32 | 16.17 | 16.57 | 3.93 |
| 7463.5 | 10.5 | 4.70 | 18.10 | 14.65 | 2.54 |
| 7758.5 | 20.5 | 7.85 | 27.24 | 21.64 | 3.27 |
| 8053.5 | 30.5 | 12.92 | 42.92 | 37.89 | 6.27 |
| 8201.1 | 40.5 | 12.88 | 42.75 | 38.06 | 6.30 |
| 8348.6 | 50.5 | 12.93 | 42.01 | 38.43 | 6.64 |
| 8480.3 | 60.5 | 12.88 | 41.95 | 38.42 | 6.75 |
| 8593.9 | 70.5 | 12.91 | 41.69 | 38.49 | 6.90 |
| 8707.5 | 80.5 | 12.88 | 40.99 | 38.85 | 7.28 |
| 8821.1 | 90.5 | 12.70 | 39.97 | 39.45 | 7.88 |
| 8934.6 | 100.5 | 12.42 | 39.86 | 39.65 | 8.08 |
| 9029.1 | 110.5 | 11.97 | 38.96 | 40.23 | 8.84 |
| 9078.9 | 120.5 | 11.62 | 38.26 | 40.86 | 9.25 |
| 9128.8 | 130.5 | 11.34 | 37.85 | 41.35 | 9.46 |
| 9178.6 | 140.5 | 11.07 | 37.41 | 41.87 | 9.65 |
| 9228.4 | 150.5 | 10.77 | 36.59 | 42.49 | 10.14 |
| 9278.2 | 160.5 | 10.72 | 36.28 | 42.46 | 10.55 |
| 9360.2 | 170.5 | 10.54 | 35.89 | 42.38 | 11.19 |
| 9455.9 | 180.5 | 10.34 | 35.09 | 42.51 | 12.06 |
| 9551.7 | 190.5 | 10.17 | 34.26 | 42.70 | 12.88 |
| 9647.4 | 200.5 | 8.08 | 27.03 | 34.19 | 10.71 |
| 9743.2 | 210.5 | 7.92 | 26.15 | 34.78 | 11.15 |
| 9838.9 | 220.5 | 7.81 | 25.09 | 35.50 | 11.60 |
| 9934.7 | 230.5 | 7.64 | 23.80 | 36.39 | 12.17 |
| 10030.4 | 240.5 | 7.63 | 23.28 | 36.83 | 12.26 |
| 10126.2 | 250.5 | 7.83 | 24.19 | 36.98 | 10.99 |
| 10184.5 | 260.5 | 8.17 | 25.24 | 36.68 | 9.91 |
| 10217.9 | 270.5 | 8.72 | 27.37 | 35.82 | 8.09 |
| 10251.3 | 280.5 | 11.97 | 37.28 | 42.82 | 7.92 |
| 10284.6 | 290.5 | 12.46 | 38.37 | 41.82 | 7.35 |
| 10318.0 | 295.5 | 10.20 | 31.41 | 32.93 | 5.45 |
| 10334.7 | 300.5 | 7.84 | 23.99 | 24.24 | 3.92 |
| 10351.4 | 302.5 | 8.02 | 24.79 | 23.62 | 3.57 |
| 10358.1 | 305.5 | 5.36 | 16.72 | 15.62 | 2.29 |
| 10368.1 | 307.5 | 7.91 | 25.07 | 23.49 | 3.53 |
| 10374.8 | 310.5 | 10.07 | 32.15 | 32.18 | 5.60 |
| 10384.8 | 315.5 | 9.60 | 30.83 | 32.91 | 6.67 |
| 10406.9 | 320.5 | 9.62 | 30.36 | 33.30 | 6.73 |
| 10451.1 | 330.5 | 9.50 | 29.76 | 34.03 | 6.72 |
| 10483.2 | 340.5 | 9.46 | 29.63 | 34.13 | 6.78 |
| 10509.1 | 350.5 | 9.56 | 29.86 | 34.04 | 6.55 |

| Age (cal yrs BP) | Mid-point depth (cm) | 0 - 2 $\mu$m | 2 - 10 $\mu$m | 10 - 63 $\mu$m | 63 - 2500$\mu$m |
|---|---|---|---|---|---|
| 10535.0 | 360.5 | 11.73 | 36.48 | 43.15 | 8.64 |
| 10560.9 | 365.5 | 11.65 | 36.52 | 43.08 | 8.75 |
| 10579.0 | 367.5 | 11.39 | 35.57 | 43.72 | 9.32 |
| 10586.7 | 370.5 | 11.12 | 34.75 | 44.70 | 9.43 |
| 10591.9 | 372.5 | 10.80 | 34.24 | 45.20 | 9.76 |
| 10599.7 | 375.5 | 10.57 | 33.91 | 45.69 | 9.82 |
| 10612.6 | 380.5 | 10.40 | 33.20 | 46.16 | 10.24 |
| 10638.5 | 390.5 | 10.40 | 34.68 | 45.55 | 9.36 |
| 10664.4 | 400.5 | 10.71 | 35.43 | 45.17 | 8.69 |
| 10691.4 | 410.5 | 11.02 | 36.80 | 44.20 | 7.98 |
| 10719.0 | 420.5 | 11.37 | 37.41 | 43.65 | 7.57 |
| 10746.7 | 430.5 | 9.26 | 30.66 | 34.58 | 5.50 |
| 10752.2 | 432.5 | 9.45 | 29.86 | 34.65 | 6.05 |
| 10760.5 | 435.5 | 7.10 | 22.70 | 25.55 | 4.65 |
| 10766.0 | 437.5 | 7.25 | 22.51 | 25.40 | 4.84 |
| 10774.3 | 440.5 | 9.60 | 29.83 | 34.08 | 6.48 |
| 10779.8 | 442.5 | 11.78 | 37.86 | 42.91 | 7.45 |
| 10788.1 | 445.5 | 11.81 | 38.08 | 43.08 | 7.03 |
| 10793.6 | 447.5 | 11.87 | 38.69 | 43.36 | 6.08 |
| 10801.9 | 450.5 | 11.96 | 39.58 | 42.84 | 5.62 |
| 10807.4 | 452.5 | 9.77 | 31.63 | 34.33 | 4.27 |
| 10815.7 | 455.5 | 10.07 | 33.05 | 33.22 | 3.66 |
| 10828.3 | 460.5 | 10.10 | 33.75 | 32.76 | 3.39 |
| 10852.3 | 470.5 | 10.21 | 34.75 | 31.67 | 3.36 |
| 10876.2 | 480.5 | 13.47 | 45.71 | 37.37 | 3.45 |
| 10900.2 | 490.5 | 13.81 | 47.02 | 36.23 | 2.95 |
| 10927.0 | 500.5 | 14.37 | 48.60 | 34.67 | 2.36 |
| 10954.0 | 510.5 | 14.76 | 50.21 | 33.06 | 1.97 |
| 10981.1 | 520.5 | 11.96 | 40.88 | 25.80 | 1.36 |
| 11008.2 | 530.5 | 9.05 | 30.99 | 19.07 | 0.89 |
| 11035.2 | 540.5 | 6.10 | 20.88 | 12.49 | 0.53 |
| 11062.3 | 550.5 | 3.00 | 10.60 | 6.12 | 0.28 |

# Appendix B
# Diatom data

| Mid-point depth( cm) | D. confervacea | F. cylindrus | F. oceanica | T. nordenskioeldii | Thalassiosira sp. a | T. angulata | B. bathyomphala | T. proschkinensis | T. hyalina | T. gravida | T. kushirensis | C. costata | Benthic sp. | N. communis | N. kariana | Sea ice taxa | Cold water taxa |
|---|---|---|---|---|---|---|---|---|---|---|---|---|---|---|---|---|---|
| 250.5 | 36.33 | 5.33 | 11.33 | 6.00 | 2.67 | 8.33 | 2.67 | 6.33 | 4.00 | 1.67 | 3.33 | 1.33 | 2.00 | 0.67 | 0.33 | 5.33 | 6.00 |
| 260.5 | 33.00 | 6.67 | 11.33 | 7.00 | 7.33 | 5.67 | 2.00 | 5.67 | 2.67 | 0.33 | 1.67 | 2.33 | 3.33 | 0.67 | 0.67 | 7.33 | 3.67 |
| 270.5 | 34.00 | 9.33 | 9.67 | 8.33 | 12.00 | 3.00 | 2.67 | 4.00 | 4.00 | 0.67 | 1.00 | 1.00 | 1.67 | 0.33 | 1.67 | 9.33 | 3.67 |
| 280.5 | 24.00 | 7.67 | 12.67 | 12.00 | 7.67 | 6.33 | 2.67 | 3.33 | 5.33 | 1.67 | 1.67 | 0.33 | 0.00 | 3.67 | 2.00 | 8.00 | 4.33 |
| 290.5 | 32.33 | 4.67 | 11.00 | 9.00 | 10.33 | 4.00 | 2.33 | 3.67 | 2.00 | 0.00 | 1.67 | 2.00 | 1.67 | 1.67 | 1.00 | 7.33 | 4.00 |
| 295.5 | 34.33 | 5.67 | 12.33 | 9.33 | 0.00 | 5.33 | 5.33 | 5.33 | 3.33 | 4.67 | 1.33 | 3.00 | 0.00 | 0.00 | 1.00 | 6.00 | 6.67 |
| 300.5 | 48.67 | 5.00 | 8.67 | 3.67 | 2.00 | 3.00 | 0.67 | 1.33 | 0.67 | 3.00 | 3.67 | 4.33 | 3.00 | 1.00 | 0.67 | 7.00 | 4.33 |
| 302.5 | 40.00 | 5.67 | 10.33 | 4.33 | 5.33 | 3.33 | 1.67 | 1.67 | 1.67 | 3.33 | 2.33 | 1.67 | 3.33 | 0.00 | 1.33 | 7.00 | 4.00 |
| 305.5 | 44.33 | 3.67 | 11.67 | 5.33 | 4.00 | 3.67 | 6.00 | 1.33 | 1.33 | 5.00 | 2.33 | 2.67 | 1.67 | 0.00 | 1.00 | 3.67 | 8.33 |
| 307.5 | 37.67 | 4.33 | 11.00 | 8.67 | 2.67 | 3.33 | 6.67 | 0.67 | 1.67 | 4.00 | 4.33 | 2.67 | 1.33 | 0.00 | 0.67 | 4.33 | 11.00 |
| 320.5 | 45.67 | 5.67 | 8.33 | 4.67 | 7.00 | 4.00 | 3.00 | 2.33 | 0.00 | 0.67 | 1.67 | 2.67 | 2.00 | 0.00 | 0.67 | 7.00 | 4.67 |
| 330.5 | 36.33 | 3.67 | 9.67 | 6.33 | 5.67 | 2.67 | 1.67 | 3.33 | 3.00 | 1.33 | 1.67 | 3.33 | 4.00 | 0.00 | 0.33 | 6.00 | 3.33 |
| 340.5 | 38.33 | 6.33 | 10.67 | 6.67 | 1.33 | 4.33 | 3.00 | 3.67 | 5.67 | 1.33 | 2.33 | 3.67 | 0.00 | 0.00 | 3.33 | 6.33 | 5.33 |
| 350.5 | 60.00 | 7.00 | 4.00 | 4.67 | 3.00 | 4.00 | 1.67 | 2.33 | 3.67 | 0.33 | 1.00 | 0.67 | 0.00 | 0.00 | 0.33 | 8.33 | 2.67 |
| 360.5 | 37.33 | 19.00 | 6.33 | 8.67 | 0.00 | 3.67 | 2.33 | 5.00 | 3.33 | 1.00 | 1.33 | 1.33 | 3.67 | 0.00 | 0.67 | 19.00 | 3.67 |

All data presented as % of total diatom abundance


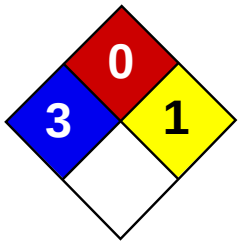



# Material Safety Data Sheet
## Hydrochloric acid MSDS

## Section 1: Chemical Product and Company Identification

**Product Name:** Hydrochloric acid

**Catalog Codes:** SLH1462, SLH3154

**CAS#:** Mixture.

**RTECS:** MW4025000

**TSCA:** TSCA 8(b) inventory: Hydrochloric acid

**CI#:** Not applicable.

**Synonym:** Hydrochloric Acid; Muriatic Acid

**Chemical Name:** Not applicable.

**Chemical Formula:** Not applicable.

**Contact Information:**

**Sciencelab.com, Inc.**
14025 Smith Rd.
Houston, Texas 77396

US Sales: **1-800-901-7247**
International Sales: **1-281-441-4400**

Order Online: ScienceLab.com

**CHEMTREC (24HR Emergency Telephone), call:**
1-800-424-9300

**International CHEMTREC, call:** 1-703-527-3887

**For non-emergency assistance, call:** 1-281-441-4400

## Section 2: Composition and Information on Ingredients

**Composition:**

| Name | CAS # | % by Weight |
|---|---|---|
| Hydrogen chloride | 7647-01-0 | 20-38 |
| Water | 7732-18-5 | 62-80 |

**Toxicological Data on Ingredients:** Hydrogen chloride: GAS (LC50): Acute: 4701 ppm 0.5 hours [Rat].

## Section 3: Hazards Identification

**Potential Acute Health Effects:**
Very hazardous in case of skin contact (corrosive, irritant, permeator), of eye contact (irritant, corrosive), of ingestion, . Slightly hazardous in case of inhalation (lung sensitizer). Non-corrosive for lungs. Liquid or spray mist may produce tissue damage particularly on mucous membranes of eyes, mouth and respiratory tract. Skin contact may produce burns. Inhalation of the spray mist may produce severe irritation of respiratory tract, characterized by coughing, choking, or shortness of breath. Severe over-exposure can result in death. Inflammation of the eye is characterized by redness, watering, and itching. Skin inflammation is characterized by itching, scaling, reddening, or, occasionally, blistering.

**Potential Chronic Health Effects:**
Slightly hazardous in case of skin contact (sensitizer). CARCINOGENIC EFFECTS: Classified 3 (Not classifiable for human.) by IARC [Hydrochloric acid]. MUTAGENIC EFFECTS: Not available. TERATOGENIC EFFECTS: Not available. DEVELOPMENTAL TOXICITY: Not available. The substance may be toxic to kidneys, liver, mucous membranes, upper respiratory tract, skin, eyes, Circulatory System, teeth. Repeated or prolonged exposure to the substance can produce target

organs damage. Repeated or prolonged contact with spray mist may produce chronic eye irritation and severe skin irritation. Repeated or prolonged exposure to spray mist may produce respiratory tract irritation leading to frequent attacks of bronchial infection. Repeated exposure to a highly toxic material may produce general deterioration of health by an accumulation in one or many human organs.

## Section 4: First Aid Measures

**Eye Contact:**
Check for and remove any contact lenses. In case of contact, immediately flush eyes with plenty of water for at least 15 minutes. Cold water may be used. Get medical attention immediately.

**Skin Contact:**
In case of contact, immediately flush skin with plenty of water for at least 15 minutes while removing contaminated clothing and shoes. Cover the irritated skin with an emollient. Cold water may be used.Wash clothing before reuse. Thoroughly clean shoes before reuse. Get medical attention immediately.

**Serious Skin Contact:**
Wash with a disinfectant soap and cover the contaminated skin with an anti-bacterial cream. Seek immediate medical attention.

**Inhalation:**
If inhaled, remove to fresh air. If not breathing, give artificial respiration. If breathing is difficult, give oxygen. Get medical attention immediately.

**Serious Inhalation:**
Evacuate the victim to a safe area as soon as possible. Loosen tight clothing such as a collar, tie, belt or waistband. If breathing is difficult, administer oxygen. If the victim is not breathing, perform mouth-to-mouth resuscitation. WARNING: It may be hazardous to the person providing aid to give mouth-to-mouth resuscitation when the inhaled material is toxic, infectious or corrosive. Seek immediate medical attention.

**Ingestion:**
If swallowed, do not induce vomiting unless directed to do so by medical personnel. Never give anything by mouth to an unconscious person. Loosen tight clothing such as a collar, tie, belt or waistband. Get medical attention immediately.

**Serious Ingestion:** Not available.

## Section 5: Fire and Explosion Data

**Flammability of the Product:** Non-flammable.

**Auto-Ignition Temperature:** Not applicable.

**Flash Points:** Not applicable.

**Flammable Limits:** Not applicable.

**Products of Combustion:** Not available.

**Fire Hazards in Presence of Various Substances:** of metals

**Explosion Hazards in Presence of Various Substances:** Non-explosive in presence of open flames and sparks, of shocks.

**Fire Fighting Media and Instructions:** Not applicable.

**Special Remarks on Fire Hazards:**
Non combustible. Calcium carbide reacts with hydrogen chloride gas with incandescence. Uranium phosphide reacts with hydrochloric acid to release spontaneously flammable phosphine. Rubidium acetylene carbides burns with slightly warm hydrochloric acid. Lithium silicide in contact with hydrogen chloride becomes incandescent. When dilute hydrochloric acid is used, gas spontaneously flammable in air is evolved. Magnesium boride treated with concentrated hydrochloric acid produces spontaneously flammble gas. Cesium acetylene carbide burns hydrogen chloride gas. Cesium carbide ignites in contact with hydrochloric acid unless acid is dilute. Reacts with most metals to produce flammable Hydrodgen gas.

**Special Remarks on Explosion Hazards:**

Hydrogen chloride in contact with the following can cause an explosion, ignition on contact, or other violent/vigorous reaction: Acetic anhydride AgClO + CCl4 Alcohols + hydrogen cyanide, Aluminum Aluminum-titanium alloys (with HCl vapor), 2-Amino ethanol, Ammonium hydroxide, Calcium carbide Ca3P2 Chlorine + dinitroanilines (evolves gas), Chlorosulfonic acid Cesium carbide Cesium acetylene carbide, 1,1-Difluoroethylene Ethylene diamine Ethylene imine, Fluorine, HClO4 Hexalithium disilicide H2SO4 Metal acetylides or carbides, Magnesium boride, Mercuric sulfate, Oleum, Potassium permanganate, beta-Propiolactone Propylene oxide Rubidium carbide, Rubidium, acetylene carbide Sodium (with aqueous HCl), Sodium hydroxide Sodium tetraselenium, Sulfonic acid, Tetraselenium tetranitride, U3P4 , Vinyl acetate. Silver perchlorate with carbon tetrachloride in the presence of hydrochloric acid produces trichloromethyl perchlorate which detonates at 40 deg. C.

## Section 6: Accidental Release Measures

**Small Spill:**
Dilute with water and mop up, or absorb with an inert dry material and place in an appropriate waste disposal container. If necessary: Neutralize the residue with a dilute solution of sodium carbonate.

**Large Spill:**
Corrosive liquid. Poisonous liquid. Stop leak if without risk. Absorb with DRY earth, sand or other non-combustible material. Do not get water inside container. Do not touch spilled material. Use water spray curtain to divert vapor drift. Use water spray to reduce vapors. Prevent entry into sewers, basements or confined areas; dike if needed. Call for assistance on disposal. Neutralize the residue with a dilute solution of sodium carbonate. Be careful that the product is not present at a concentration level above TLV. Check TLV on the MSDS and with local authorities.

## Section 7: Handling and Storage

**Precautions:**
Keep locked up.. Keep container dry. Do not ingest. Do not breathe gas/fumes/ vapor/spray. Never add water to this product. In case of insufficient ventilation, wear suitable respiratory equipment. If ingested, seek medical advice immediately and show the container or the label. Avoid contact with skin and eyes. Keep away from incompatibles such as oxidizing agents, organic materials, metals, alkalis, moisture. May corrode metallic surfaces. Store in a metallic or coated fiberboard drum using a strong polyethylene inner package.

**Storage:** Keep container tightly closed. Keep container in a cool, well-ventilated area.

## Section 8: Exposure Controls/Personal Protection

**Engineering Controls:**
Provide exhaust ventilation or other engineering controls to keep the airborne concentrations of vapors below their respective threshold limit value. Ensure that eyewash stations and safety showers are proximal to the work-station location.

**Personal Protection:**
Face shield. Full suit. Vapor respirator. Be sure to use an approved/certified respirator or equivalent. Gloves. Boots.

**Personal Protection in Case of a Large Spill:**
Splash goggles. Full suit. Vapor respirator. Boots. Gloves. A self contained breathing apparatus should be used to avoid inhalation of the product. Suggested protective clothing might not be sufficient; consult a specialist BEFORE handling this product.

**Exposure Limits:**
CEIL: 5 (ppm) from OSHA (PEL) [United States] CEIL: 7 (mg/m3) from OSHA (PEL) [United States] CEIL: 5 from NIOSH CEIL: 7 (mg/m3) from NIOSH TWA: 1 STEL: 5 (ppm) [United Kingdom (UK)] TWA: 2 STEL: 8 (mg/m3) [United Kingdom (UK)]Consult local authorities for acceptable exposure limits.

## Section 9: Physical and Chemical Properties

**Physical state and appearance:** Liquid.

**Odor:** Pungent. Irritating (Strong.)

**Taste:** Not available.

**Molecular Weight:** Not applicable.

**Color:** Colorless to light yellow.

**pH (1% soln/water):** Acidic.

**Boiling Point:**
108.58 C @ 760 mm Hg (for 20.22% HCl in water) 83 C @ 760 mm Hg (for 31% HCl in water) 50.5 C (for 37% HCl in water)

**Melting Point:**
-62.25°C (-80°F) (20.69% HCl in water) -46.2 C (31.24% HCl in water) -25.4 C (39.17% HCl in water)

**Critical Temperature:** Not available.

**Specific Gravity:**
1.1- 1.19 (Water = 1) 1.10 (20%and 22% HCl solutions) 1.12 (24% HCl solution) 1.15 (29.57% HCl solution) 1.16 (32% HCl solution) 1.19 (37% and 38%HCl solutions)

**Vapor Pressure:** 16 kPa (@ 20°C) average

**Vapor Density:** 1.267 (Air = 1)

**Volatility:** Not available.

**Odor Threshold:** 0.25 to 10 ppm

**Water/Oil Dist. Coeff.:** Not available.

**Ionicity (in Water):** Not available.

**Dispersion Properties:** See solubility in water, diethyl ether.

**Solubility:** Soluble in cold water, hot water, diethyl ether.

## Section 10: Stability and Reactivity Data

**Stability:** The product is stable.

**Instability Temperature:** Not available.

**Conditions of Instability:** Incompatible materials, water

**Incompatibility with various substances:**
Highly reactive with metals. Reactive with oxidizing agents, organic materials, alkalis, water.

**Corrosivity:**
Extremely corrosive in presence of aluminum, of copper, of stainless steel(304), of stainless steel(316). Non-corrosive in presence of glass.

**Special Remarks on Reactivity:**
Reacts with water especially when water is added to the product. Absorption of gaseous hydrogen chloride on mercuric sulfate becomes violent @ 125 deg. C. Sodium reacts very violently with gaseous hydrogen chloride. Calcium phosphide and hydrochloric acid undergo very energetic reaction. It reacts with oxidizers releasing chlorine gas. Incompatible with, alkali metals, carbides, borides, metal oxides, vinyl acetate, acetylides, sulphides, phosphides, cyanides, carbonates. Reacts with most metals to produce flammable Hydrogen gas. Reacts violently (moderate reaction with heat of evolution) with water especially when water is added to the product. Isolate hydrogen chloride from heat, direct sunlight, alkalies (reacts vigorously), organic materials, and oxidizers (especially nitric acid and chlorates), amines, metals, copper and alloys (e.g. brass), hydroxides, zinc (galvanized materials), lithium silicide (incandescence), sulfuric acid(increase in temperature and pressure) Hydrogen chloride gas is emitted when this product is in contact with sulfuric acid. Adsorption of Hydrochloric Acid onto silicon dioxide results in exothmeric reaction. Hydrogen chloride causes aldehydes and epoxides to violently polymerize. Hydrogen chloride or Hydrochloric Acid in contact with the folloiwng can cause explosion or ignition on contact or

**Special Remarks on Corrosivity:**

Highly corrosive. Incompatible with copper and copper alloys. It attacks nearly all metals (mercury, gold, platinium, tantalum, silver, and certain alloys are exceptions). It is one of the most corrosive of the nonoxidizing acids in contact with copper alloys. No corrosivity data on zinc, steel. Severe Corrosive effect on brass and bronze

**Polymerization:** Will not occur.

## Section 11: Toxicological Information

**Routes of Entry:** Absorbed through skin. Dermal contact. Eye contact. Inhalation.

**Toxicity to Animals:**
Acute oral toxicity (LD50): 900 mg/kg [Rabbit]. Acute toxicity of the vapor (LC50): 1108 ppm, 1 hours [Mouse]. Acute toxicity of the vapor (LC50): 3124 ppm, 1 hours [Rat].

**Chronic Effects on Humans:**
CARCINOGENIC EFFECTS: Classified 3 (Not classifiable for human.) by IARC [Hydrochloric acid]. May cause damage to the following organs: kidneys, liver, mucous membranes, upper respiratory tract, skin, eyes, Circulatory System, teeth.

**Other Toxic Effects on Humans:**
Very hazardous in case of skin contact (corrosive, irritant, permeator), of ingestion, . Hazardous in case of eye contact (corrosive), of inhalation (lung corrosive).

**Special Remarks on Toxicity to Animals:**
Lowest Published Lethal Doses (LDL/LCL) LDL [Man] -Route: Oral; 2857 ug/kg LCL [Human] - Route: Inhalation; Dose: 1300 ppm/30M LCL [Rabbit] - Route: Inhalation; Dose: 4413 ppm/30M

**Special Remarks on Chronic Effects on Humans:**
May cause adverse reproductive effects (fetoxicity). May affect genetic material.

**Special Remarks on other Toxic Effects on Humans:**
Acute Potential Health Effects: Skin: Corrosive. Causes severe skin irritation and burns. Eyes: Corrosive. Causes severe eye irritation/conjuntivitis, burns, corneal necrosis. Inhalation: May be fatal if inhaled. Material is extremely destructive to tissue of the mucous membranes and upper respiratory tract. Inhalation of hydrochloric acid fumes produces nose, throat, and larryngeal burning, and irritation, pain and inflammation, coughing, sneezing, choking sensation, hoarseness, laryngeal spasms, upper respiratory tract edema, chest pains, as well has headache, and palpitations. Inhalation of high concentrations can result in corrosive burns, necrosis of bronchial epithelium, constriction of the larynx and bronchi, nasospetal perforation, glottal closure,  occur, particularly if exposure is prolonged. May affect the liver. Ingestion: May be fatal if swallowed. Causes irritation and burning, ulceration, or perforation of the gastrointestinal tract and resultant peritonitis, gastric hemorrhage and infection. Can also cause nausea, vomitting (with "coffee ground" emesis), diarrhea, thirst, difficulty swallowing, salivation, chills, fever, uneasiness, shock, strictures and stenosis (esophogeal, gastric, pyloric). May affect behavior (excitement), the cardiovascular system (weak rapid pulse, tachycardia), respiration (shallow respiration), and urinary system (kidneys- renal failure, nephritis). Acute exposure via inhalation or ingestion can also cause erosion of tooth enamel. Chronic Potential Health Effects: dyspnea, bronchitis. Chemical pneumonitis and pulmonary edema can also

## Section 12: Ecological Information

**Ecotoxicity:** Not available.

**BOD5 and COD:** Not available.

**Products of Biodegradation:**
Possibly hazardous short term degradation products are not likely. However, long term degradation products may arise.

**Toxicity of the Products of Biodegradation:** The products of degradation are less toxic than the product itself.

**Special Remarks on the Products of Biodegradation:** Not available.

## Section 13: Disposal Considerations

**Waste Disposal:**

Waste must be disposed of in accordance with federal, state and local environmental control regulations.

## Section 14: Transport Information

**DOT Classification:** Class 8: Corrosive material

**Identification:** : Hydrochloric acid, solution UNNA: 1789 PG: II

**Special Provisions for Transport:** Not available.

## Section 15: Other Regulatory Information

**Federal and State Regulations:**
Connecticut hazardous material survey.: Hydrochloric acid Illinois toxic substances disclosure to employee act: Hydrochloric acid Illinois chemical safety act: Hydrochloric acid New York release reporting list: Hydrochloric acid Rhode Island RTK hazardous substances: Hydrochloric acid Pennsylvania RTK: Hydrochloric acid Minnesota: Hydrochloric acid Massachusetts RTK: Hydrochloric acid Massachusetts spill list: Hydrochloric acid New Jersey: Hydrochloric acid New Jersey spill list: Hydrochloric acid Louisiana RTK reporting list: Hydrochloric acid Louisiana spill reporting: Hydrochloric acid California Director's List of Hazardous Substances: Hydrochloric acid TSCA 8(b) inventory: Hydrochloric acid TSCA 4(a) proposed test rules: Hydrochloric acid SARA 302/304/311/312 extremely hazardous substances: Hydrochloric acid SARA 313 toxic chemical notification and release reporting: Hydrochloric acid CERCLA: Hazardous substances.: Hydrochloric acid: 5000 lbs. (2268 kg)

**Other Regulations:**
OSHA: Hazardous by definition of Hazard Communication Standard (29 CFR 1910.1200). EINECS: This product is on the European Inventory of Existing Commercial Chemical Substances.

**Other Classifications:**

**WHMIS (Canada):**
CLASS D-2A: Material causing other toxic effects (VERY TOXIC). CLASS E: Corrosive liquid.

**DSCL (EEC):**
R34- Causes burns. R37- Irritating to respiratory system. S26- In case of contact with eyes, rinse immediately with plenty of water and seek medical advice. S45- In case of accident or if you feel unwell, seek medical advice immediately (show the label where possible).

**HMIS (U.S.A.):**

**Health Hazard:** 3

**Fire Hazard:** 0

**Reactivity:** 1

**Personal Protection:**

**National Fire Protection Association (U.S.A.):**

**Health:** 3

**Flammability:** 0

**Reactivity:** 1

**Specific hazard:**

**Protective Equipment:**
Gloves. Full suit. Vapor respirator. Be sure to use an approved/certified respirator or equivalent. Wear appropriate respirator when ventilation is inadequate. Face shield.

## Section 16: Other Information

**References:**
-Hawley, G.G.. The Condensed Chemical Dictionary, 11e ed., New York N.Y., Van Nostrand Reinold, 1987. -SAX, N.I. Dangerous Properties of Indutrial Materials. Toronto, Van Nostrand Reinold, 6e ed. 1984. -The Sigma-Aldrich Library of Chemical Safety Data, Edition II. -Guide de la loi et du règlement sur le transport des marchandises dangeureuses au canada. Centre de conformité internatinal Ltée. 1986.

**Other Special Considerations:** Not available.

**Created:** 10/09/2005 05:45 PM

**Last Updated:** 05/21/2013 12:00 PM


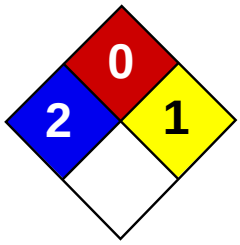



# Material Safety Data Sheet
## Hydrogen Peroxide 30% MSDS

## Section 1: Chemical Product and Company Identification

**Product Name:** Hydrogen Peroxide 30%

**Catalog Codes:** SLH1552

**CAS#:** Mixture.

**RTECS:** Not applicable.

**TSCA:** TSCA 8(b) inventory: Water; Hydrogen Peroxide

**CI#:** Not applicable.

**Synonym:** Hydrogen Peroxide 30%

**Chemical Name:** Not applicable.

**Chemical Formula:** Not applicable.

**Contact Information:**

**Sciencelab.com, Inc.**
14025 Smith Rd.
Houston, Texas 77396

US Sales: **1-800-901-7247**
International Sales: **1-281-441-4400**

Order Online: ScienceLab.com

**CHEMTREC (24HR Emergency Telephone), call:**
1-800-424-9300

**International CHEMTREC, call:** 1-703-527-3887

**For non-emergency assistance, call:** 1-281-441-4400

## Section 2: Composition and Information on Ingredients

**Composition:**

| Name | CAS # | % by Weight |
|---|---|---|
| Water | 7732-18-5 | 70 |
| Hydrogen Peroxide | 7722-84-1 | 30 |

**Toxicological Data on Ingredients:** Hydrogen Peroxide: ORAL (LD50): Acute: 2000 mg/kg [Mouse]. DERMAL (LD50): Acute: 4060 mg/kg [Rat]. 2000 mg/kg [ pig]. VAPOR (LC50): Acute: 2000 mg/m 4 hours [Rat].

## Section 3: Hazards Identification

**Potential Acute Health Effects:**
Very hazardous in case of skin contact (irritant), of eye contact (irritant). Hazardous in case of skin contact (corrosive), of eye contact (corrosive), of ingestion, . Slightly hazardous in case of inhalation (lung sensitizer). Liquid or spray mist may produce tissue damage particularly on mucous membranes of eyes, mouth and respiratory tract. Skin contact may produce burns. Inhalation of the spray mist may produce severe irritation of respiratory tract, characterized by coughing, choking, or shortness of breath. Prolonged exposure may result in skin burns and ulcerations. Over-exposure by inhalation may cause respiratory irritation. Inflammation of the eye is characterized by redness, watering, and itching. Skin inflammation is characterized by itching, scaling, reddening, or, occasionally, blistering.

**Potential Chronic Health Effects:**
CARCINOGENIC EFFECTS: Not available. MUTAGENIC EFFECTS: Not available. TERATOGENIC EFFECTS: Not available. DEVELOPMENTAL TOXICITY: Not available. The substance is toxic to lungs, mucous membranes. Repeated or prolonged exposure to the substance can produce target organs damage.

## Section 4: First Aid Measures

**Eye Contact:**
Check for and remove any contact lenses. In case of contact, immediately flush eyes with plenty of water for at least 15 minutes. Cold water may be used. Get medical attention immediately.

**Skin Contact:**
In case of contact, immediately flush skin with plenty of water for at least 15 minutes while removing contaminated clothing and shoes. Cover the irritated skin with an emollient. Cold water may be used.Wash clothing before reuse. Thoroughly clean shoes before reuse. Get medical attention immediately.

**Serious Skin Contact:**
Wash with a disinfectant soap and cover the contaminated skin with an anti-bacterial cream. Seek immediate medical attention.

**Inhalation:**
If inhaled, remove to fresh air. If not breathing, give artificial respiration. If breathing is difficult, give oxygen. Get medical attention immediately.

**Serious Inhalation:**
Evacuate the victim to a safe area as soon as possible. Loosen tight clothing such as a collar, tie, belt or waistband. If breathing is difficult, administer oxygen. If the victim is not breathing, perform mouth-to-mouth resuscitation. WARNING: It may be hazardous to the person providing aid to give mouth-to-mouth resuscitation when the inhaled material is toxic, infectious or corrosive. Seek immediate medical attention.

**Ingestion:**
Do NOT induce vomiting unless directed to do so by medical personnel. Never give anything by mouth to an unconscious person. Loosen tight clothing such as a collar, tie, belt or waistband. Get medical attention if symptoms appear.

**Serious Ingestion:** Not available.

## Section 5: Fire and Explosion Data

**Flammability of the Product:** Non-flammable.

**Auto-Ignition Temperature:** Not applicable.

**Flash Points:** Not applicable.

**Flammable Limits:** Not applicable.

**Products of Combustion:** Not available.

**Fire Hazards in Presence of Various Substances:** combustible materials

**Explosion Hazards in Presence of Various Substances:** Slightly explosive in presence of open flames and sparks, of heat, of organic materials, of metals, of acids.

**Fire Fighting Media and Instructions:**
Fire: Small fires: Use water. Do not use dry chemicals or foams. CO2, or Halon may provide limited control. Large fires: Flood fire area with water from a distance. Move containers from fire area if you can do it without risk. Do not move cargo or vehicle if cargo has been exposed to heat. Fight fire from maximum distance or use unmanned hose holders or monitor nozzles. Cool containers with flooding quantities of water until well after fire is out. ALWAYS stay away from tanks engulfed in fire. For massive fire, use unmanned hose holders or monitor nozzles; if this is impossible, withdraw from area and let fire burn. / Hydrogen peroxide, aqueous solution, with not less than 8% but less than 20% Hydrogen peroxide; Hydrogen peroxide, aqueous solution, with not less than 20% but not more than 60% Hydrogen peroxide (stabilized as necessary)/ [QC Reviewed] [U.S. Department of Transportation. 2000 Emergency Response Guidebook. RSPA P 5800.8 Edition. Washington, D.C: U.S. Government Printing Office, 2000,p. G-140]

**Special Remarks on Fire Hazards:**
Most cellulose (wood, cotton) materials contain enough catalyst to cause spontaneous ignition with 90% Hydrogen Peroxide. Hydrogen Peroxide is a strong oxider. It is not flammable itself, but it can cause spontaneous combustion of flammable materials and continued support of the combustion because it liberates oxygen as it decomposes. Hydrogen peroxide mixed with magnesium and a trace of magnesium dioxide will ignite immediately.

**Special Remarks on Explosion Hazards:**

Soluble fuels (acetone, ethanol, glycerol) will detonate on a mixture with peroxide over 30% concentration, the violence increasing with concentration. Explosive with acetic acid, acetic anhydride, acetone, alcohols, carboxylic acids, nitrogen containing bases, As2S3, Cl2 + KOH, FeS, FeSO4 + 2 methylpryidine + H2SO4, nitric acid, potassium permanganate, P2O5, H2Se, Alcohols + H2SO4, Alcohols + tin chloride, Antimoy trisulfide, chlorosulfonic acid, Aromatic hydrocarbons + trifluoroacetic acid, Azeliac acid + sulfuric acid (above 45 C), Benzenesulfonic anhydride, tert-butanol + sulfuric acid, Hydrazine, Sulfuric acid, Sodium iodate, Tetrahydrothiophene, Thiodiglycol, Mercurous oxide, mercuric oxide, Lead dioxide, Lead oxide, Manganese dioxide, Lead sulfide, Gallium + HCl, Ketenes + nitric acid, Iron (II) sulfate + 2-methylpyridine + sulfuric acid, Iron (II) sulfate + nitric acid, + sodium carboxymethylcellulose (when evaporated), Vinyl acetate, trioxane, water + oxygenated compounds (eg: acetaldehyde, acetic acid, acetone, ethanol, formaldehyde, formic acid, methanol, 2-propanol, propionaldehyde), organic compounds. Beware: Many mixitures of hydrogen peroxide and organic materials may not explode upon contact. However, the resulting combination is detonatable either upon catching fire or by impact. EXPLOSION HAZARD: SEVERE, WHEN HIGHLY CONCENTRATED OR PURE H2O2 IS EXPOSED TO HEAT, MECHANICAL IMPACT, OR CAUSED TO DECOMPOSE CATALYTICALLY BY METALS & THEIR SALTS, DUSTS & ALKALIES. ANOTHER SOURCE OF HYDROGEN PEROXIDE EXPLOSIONS IS FROM SEALING THE MATERIAL IN STRONG CONTAINERS. UNDER SUCH CONDITIONS EVEN GRADUAL DECOMPOSITION OF HYDROGEN PEROXIDE TO WATER + 1/2 OXYGEN CAN CAUSE LARGE PRESSURES TO BUILD UP IN THE CONTAINERS WHICH MAY BURST EXPLOSIVELY. Fire or explosion: May explode from friction, heat or contamination. These substances will accelerate burning when involved in a fire. May ignite combustibles (wood, paper, oil, clothing, etc.). Some will react explosively with hydrocarbons (fuels). Containers may explode when heated. Runoff may create fire or explosion hazard. /Hydrogen peroxide, aqueous solution, stabilized, with more than 60% Hydrogen peroxide; Hydrogen peroxide, stabilized/ [QC Reviewed] [U.S. Department of Transportation. 2000 Emergency Response Guidebook. RSPA P 5800.8 Edition. Washington, D.C: U.S. Government Printing Office, 2000,p. G-143] . Fire or explosion: These substances will accelerate burning when involved in a fire. Some may decompose explosively when heated or involved in a fire. May explode from heat or contamination. Some will react explosively with hydrocarbons (fuels). May ignite combustibles (wood, paper, oil, clothing, etc.). Containers may explode when heated. Runoff may create fire or explosion hazard. /Hydrogen peroxide, aqueous solution, with not less than 8% but less than 20% Hydrogen peroxide; Hydrogen peroxide, aqueous solution, with not less than 20% but not more than 60% Hydrogen peroxide (stabilized as necessary)/ [QC Reviewed] [U.S. Department of Transportation. 2000 Emergency Response Guidebook. RSPA P 5800.8 Edition. Washington, D.C: U.S. Government Printing Office, 2000,p. G-140] (Hydrogen Peroxide)

## Section 6: Accidental Release Measures

**Small Spill:**
Dilute with water and mop up, or absorb with an inert dry material and place in an appropriate waste disposal container.

**Large Spill:**
Corrosive liquid. Oxidizing material. Stop leak if without risk. Absorb with DRY earth, sand or other non-combustible material. Do not get water inside container. Avoid contact with a combustible material (wood, paper, oil, clothing...). Keep substance damp using water spray. Do not touch spilled material. Use water spray curtain to divert vapor drift. Prevent entry into sewers, basements or confined areas; dike if needed. Call for assistance on disposal. Be careful that the product is not present at a concentration level above TLV. Check TLV on the MSDS and with local authorities.

## Section 7: Handling and Storage

**Precautions:**
Keep locked up.. Keep container dry. Keep away from heat. Keep away from sources of ignition. Keep away from combustible material.. Do not ingest. Do not breathe gas/fumes/ vapor/spray. Never add water to this product. In case of insufficient ventilation, wear suitable respiratory equipment. If ingested, seek medical advice immediately and show the container or the label. Avoid contact with skin and eyes. Keep away from incompatibles such as oxidizing agents, reducing agents, combustible materials, organic materials, metals, acids, alkalis.

**Storage:**
Keep container tightly closed. Keep container in a cool, well-ventilated area. Separate from acids, alkalies, reducing agents and combustibles. See NFPA 43A, Code for the Storage of Liquid and Solid Oxidizers. Do not store above 8°C (46.4°F). Refrigerate Sensitive to light. Store in light-resistant containers.

## Section 8: Exposure Controls/Personal Protection

**Engineering Controls:**
Provide exhaust ventilation or other engineering controls to keep the airborne concentrations of vapors below their respective threshold limit value. Ensure that eyewash stations and safety showers are proximal to the work-station location.

**Personal Protection:**
Face shield. Full suit. Vapor respirator. Be sure to use an approved/certified respirator or equivalent. Gloves. Boots.

**Personal Protection in Case of a Large Spill:**
Splash goggles. Full suit. Vapor respirator. Boots. Gloves. A self contained breathing apparatus should be used to avoid inhalation of the product. Suggested protective clothing might not be sufficient; consult a specialist BEFORE handling this product.

**Exposure Limits:**
Hydrogen Peroxide TWA: 1 (ppm) from ACGIH (TLV) [United States] TWA: 1 (ppm) from OSHA (PEL) [United States] TWA: 1 STEL: 2 [Canada] TWA: 1.4 (mg/m3) from NIOSH TWA: 1.4 (mg/m3) from OSHA (PEL) [United States] TWA: 1 (ppm) [United Kingdom (UK)] TWA: 1.4 (mg/m3) [United Kingdom (UK)]Consult local authorities for acceptable exposure limits.

## Section 9: Physical and Chemical Properties

**Physical state and appearance:** Liquid.

**Odor:** Odorless.

**Taste:** Slightly acid. Bitter

**Molecular Weight:** Not applicable.

**Color:** Clear Colorless.

**pH (1% soln/water):** Not available

**Boiling Point:** 108°C (226.4°F)

**Melting Point:** -33°C (-27.4°F)

**Critical Temperature:** Not available.

**Specific Gravity:** 1.1 (Water = 1)

**Vapor Pressure:** 3.1 kPa (@ 20°C)

**Vapor Density:** 1.1 (Air = 1)

**Volatility:** Not available.

**Odor Threshold:** Not available.

**Water/Oil Dist. Coeff.:** Not available.

**Ionicity (in Water):** Not available.

**Dispersion Properties:** See solubility in water, diethyl ether.

**Solubility:**
Easily soluble in cold water. Soluble in diethyl ether.

## Section 10: Stability and Reactivity Data

**Stability:** The product is stable. It contains a stabilizer.

**Instability Temperature:** Not available.

**Conditions of Instability:** Excess heat, incompatible materials

**Incompatibility with various substances:** Reactive with reducing agents, combustible materials, organic materials, metals, acids, alkalis.

**Corrosivity:** Non-corrosive in presence of glass.

**Special Remarks on Reactivity:**
Light sensitive. Incompatible with reducing materials, ethers (dioxane, furfuran, tetrahydrofuran), oxidizing materials, Metals(eg. potassium, sodium lithium, iron, copper, brass, bronze, chromium, zinc, lead, silver, nickel), metal oxides (eg. cobalt oxide, iron oxide, lead oxide, lead hydroxide, manganese oxide), metal salts (eg. calcium permanganate, salts of iron), manganese, asbestos, vanadium, platinium, tungsten, molybdeum, triethylamine, palladium, sodium pyrophosphate, carboxylic acids, cyclopentadiene, formic acid, rust, ketones, sodium carbonate, alcohols, sodium borate, aniline, mercurous chloride, rust, nitric acid, sodium pyrophosphate, hexavalent chromium compounds, tetrahydrofuran, sodium fluoride organic matter, potassium permanganate, urea, chlorosulfonic acid, manganese dioxide, hydrogen selenide, charcoal, coal, sodium borate, alkalies, cyclopentadiene, glycerine, cyanides (potassium, cyanide, sodium cyanide), nitrogen compounds.. Caused to decompose catalytically by metals (in order of decreasing effectiveness): Osmium, Palladium, Platinum, Iridium, Gold, Silver, Manganese, Cobalt, Copper, Lead. Concentrated hydrogen peroxide may decompose violently or explosively in contact with iron, copper, chromium, and most other metals and their salts, and dust. (Hydrogen Peroxide)

**Special Remarks on Corrosivity:** Not available.

**Polymerization:** Will not occur.

## Section 11: Toxicological Information

**Routes of Entry:** Absorbed through skin. Eye contact.

**Toxicity to Animals:**
Acute oral toxicity (LD50): 6667 mg/kg (Mouse) (Calculated value for the mixture). Acute dermal toxicity (LD50): 6667 mg/kg ( pig) (Calculated value for the mixture).

**Chronic Effects on Humans:**
CARCINOGENIC EFFECTS: Classified A3 (Proven for animal.) by ACGIH [Hydrogen Peroxide]. Classified 3 (Not classifiable for human.) by IARC [Hydrogen Peroxide]. MUTAGENIC EFFECTS: Mutagenic for mammalian somatic cells. [Hydrogen Peroxide]. Mutagenic for bacteria and/or yeast. [Hydrogen Peroxide]. Contains material which may cause damage to the following organs: blood, upper respiratory tract, skin, eyes, central nervous system (CNS).

**Other Toxic Effects on Humans:**
Very hazardous in case of skin contact (irritant). Hazardous in case of skin contact (corrosive), of eye contact (corrosive), of ingestion, of inhalation (lung corrosive).

**Special Remarks on Toxicity to Animals:** Not available.

**Special Remarks on Chronic Effects on Humans:**
May cause cancer and may affect genetic material based on animal data. May be tumorigenic. (Hydrogen Peroxide)

**Special Remarks on other Toxic Effects on Humans:**
Acute Potential Health Effects: Skin: Causes severe skin irritation and possible burns. Absorption into skin may affect behavior/central nervous system (tremor, ataxia, convulsions), respiration (dyspnea, pulmonary emboli), brain. Eyes: Causes severe eye irritation, superficial clouding, corneal edema, and may cause burns. Inhalation: Causes respiratory tract irritation with coughing, lacrimation. May cause chemical burns to the respiratory tract. May affect behavior/Central nervous system (insomnia, headache, ataxia, nervous tremors with numb extremities) and may cause ulceration of nasal tissue, and , chemical pneumonia, unconciousness, and possible death. At high concentrations, respiratory effects may include acute lung damage, and delayed pulmonary edema. May affect blood. Ingestion: Causes gastrointestional tract irritation with nausea, vomiting, hypermotility, and diarrhea. Causes gastrointestional tract burns. May affect cardiovascular system and cause vascular collapse and damage. May affect blood (change in leukocyte count, pigmented or nucleated red blood cells). May cause difficulty in swallowing, stomach distension and possible cerebal swelling. May affect behavior/central nervous system (tetany, excitement). Chronic Potential Health Effects: Prolonged or repeated skin contact may cause dermatitis. Repeated contact may also cause corneal damage. Prolonged or repeated ingestion may affect metabolism (weight loss). Prolonged or repeated inhalation may affect respiration, blood. (Hydrogen Peroxide)

## Section 12: Ecological Information

**Ecotoxicity:** Not available.

**BOD5 and COD:** Not available.

**Products of Biodegradation:** Possibly hazardous short/long term degradation products are to be expected.

**Toxicity of the Products of Biodegradation:** The products of degradation are less toxic than the product itself.

**Special Remarks on the Products of Biodegradation:** Not available.

## Section 13: Disposal Considerations

**Waste Disposal:**
Waste must be disposed of in accordance with federal, state and local environmental control regulations.

## Section 14: Transport Information

**DOT Classification:** CLASS 5.1: Oxidizing material.

**Identification:** : Hydrogen peroxide, aqueous solution UNNA: 2014 PG: II

**Special Provisions for Transport:** Not available.

## Section 15: Other Regulatory Information

**Federal and State Regulations:**
New York acutely hazardous substances: Hydrogen Peroxide Rhode Island RTK hazardous substances: Hydrogen Peroxide Pennsylvania RTK: Hydrogen Peroxide Florida: Hydrogen Peroxide Minnesota: Hydrogen Peroxide Massachusetts RTK: Hydrogen Peroxide New Jersey: Hydrogen Peroxide TSCA 8(b) inventory: Hydrogen Peroxide SARA 302/304/311/312 extremely hazardous substances: Hydrogen Peroxide CERCLA: Hazardous substances.: Hydrogen Peroxide: 1 lbs. (0.4536 kg);

**Other Regulations:** OSHA: Hazardous by definition of Hazard Communication Standard (29 CFR 1910.1200).

**Other Classifications:**

**WHMIS (Canada):**
CLASS C: Oxidizing material. CLASS E: Corrosive liquid. CLASS F: Dangerously reactive material.

**DSCL (EEC):**

**HMIS (U.S.A.):**

**Health Hazard:** 3

**Fire Hazard:** 0

**Reactivity:** 1

**Personal Protection:**

**National Fire Protection Association (U.S.A.):**

**Health:** 2

**Flammability:** 0

**Reactivity:** 1

**Specific hazard:**

**Protective Equipment:**
Gloves. Full suit. Vapor respirator. Be sure to use an approved/certified respirator or equivalent. Wear appropriate respirator when ventilation is inadequate. Face shield.

## Section 16: Other Information

**References:** Not available.

**Other Special Considerations:** Not available.

**Created:** 10/09/2005 05:46 PM

**Last Updated:** 05/21/2013 12:00 PM


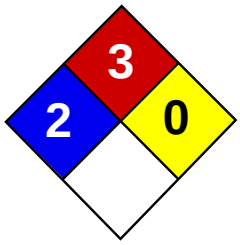


| | |
|---|---|
| Health | 2 |
| Fire | 3 |
| Reactivity | 0 |
| Personal Protection | H |

# Material Safety Data Sheet
## Toluene MSDS

## Section 1: Chemical Product and Company Identification

**Product Name:** Toluene

**Catalog Codes:** SLT2857, SLT3277

**CAS#:** 108-88-3

**RTECS:** XS5250000

**TSCA:** TSCA 8(b) inventory: Toluene

**CI#:** Not available.

**Synonym:** Toluol, Tolu-Sol; Methylbenzene; Methacide; Phenylmethane; Methylbenzol

**Chemical Name:** Toluene

**Chemical Formula:** C6-H5-CH3 or C7-H8

**Contact Information:**

**Sciencelab.com, Inc.**
14025 Smith Rd.
Houston, Texas 77396

US Sales: **1-800-901-7247**
International Sales: **1-281-441-4400**

Order Online: ScienceLab.com

**CHEMTREC (24HR Emergency Telephone), call:** 1-800-424-9300

**International CHEMTREC, call:** 1-703-527-3887

**For non-emergency assistance, call:** 1-281-441-4400

## Section 2: Composition and Information on Ingredients

**Composition:**

| Name | CAS # | % by Weight |
|---|---|---|
| Toluene | 108-88-3 | 100 |

**Toxicological Data on Ingredients:** Toluene: ORAL (LD50): Acute: 636 mg/kg [Rat]. DERMAL (LD50): Acute: 14100 mg/kg [Rabbit]. VAPOR (LC50): Acute: 49000 mg/m 4 hours [Rat]. 440 ppm 24 hours [Mouse].

## Section 3: Hazards Identification

**Potential Acute Health Effects:**
Hazardous in case of skin contact (irritant), of eye contact (irritant), of ingestion, of inhalation. Slightly hazardous in case of skin contact (permeator).

**Potential Chronic Health Effects:**
CARCINOGENIC EFFECTS: A4 (Not classifiable for human or animal.) by ACGIH, 3 (Not classifiable for human.) by IARC. MUTAGENIC EFFECTS: Not available. TERATOGENIC EFFECTS: Not available. DEVELOPMENTAL TOXICITY: Not available. The substance may be toxic to blood, kidneys, the nervous system, liver, brain, central nervous system (CNS). Repeated or prolonged exposure to the substance can produce target organs damage.

## Section 4: First Aid Measures

**Eye Contact:**
Check for and remove any contact lenses. In case of contact, immediately flush eyes with plenty of water for at least 15 minutes. Get medical attention.

**Skin Contact:**
In case of contact, immediately flush skin with plenty of water. Cover the irritated skin with an emollient. Remove contaminated clothing and shoes. Wash clothing before reuse. Thoroughly clean shoes before reuse. Get medical attention.

**Serious Skin Contact:**
Wash with a disinfectant soap and cover the contaminated skin with an anti-bacterial cream. Seek immediate medical attention.

**Inhalation:**
If inhaled, remove to fresh air. If not breathing, give artificial respiration. If breathing is difficult, give oxygen. Get medical attention.

**Serious Inhalation:**
Evacuate the victim to a safe area as soon as possible. Loosen tight clothing such as a collar, tie, belt or waistband. If breathing is difficult, administer oxygen. If the victim is not breathing, perform mouth-to-mouth resuscitation. WARNING: It may be hazardous to the person providing aid to give mouth-to-mouth resuscitation when the inhaled material is toxic, infectious or corrosive. Seek medical attention.

**Ingestion:**
Do NOT induce vomiting unless directed to do so by medical personnel. Never give anything by mouth to an unconscious person. If large quantities of this material are swallowed, call a physician immediately. Loosen tight clothing such as a collar, tie, belt or waistband.

**Serious Ingestion:** Not available.

## Section 5: Fire and Explosion Data

**Flammability of the Product:** Flammable.

**Auto-Ignition Temperature:** 480°C (896°F)

**Flash Points:** CLOSED CUP: 4.4444°C (40°F). (Setaflash) OPEN CUP: 16°C (60.8°F).

**Flammable Limits:** LOWER: 1.1% UPPER: 7.1%

**Products of Combustion:** These products are carbon oxides (CO, CO2).

**Fire Hazards in Presence of Various Substances:**
Flammable in presence of open flames and sparks, of heat. Non-flammable in presence of shocks.

**Explosion Hazards in Presence of Various Substances:**
Risks of explosion of the product in presence of mechanical impact: Not available. Risks of explosion of the product in presence of static discharge: Not available.

**Fire Fighting Media and Instructions:**
Flammable liquid, insoluble in water. SMALL FIRE: Use DRY chemical powder. LARGE FIRE: Use water spray or fog.

**Special Remarks on Fire Hazards:** Not available.

**Special Remarks on Explosion Hazards:**
Toluene forms explosive reaction with 1,3-dichloro-5,5-dimethyl-2,4-imidazolididione; dinitrogen tetraoxide; concentrated nitric acid, sulfuric acid + nitric acid; N2O4; AgClO4; BrF3; Uranium hexafluoride; sulfur dichloride. Also forms an explosive mixture with tetranitromethane.

## Section 6: Accidental Release Measures

**Small Spill:** Absorb with an inert material and put the spilled material in an appropriate waste disposal.

**Large Spill:**
Toxic flammable liquid, insoluble or very slightly soluble in water. Keep away from heat. Keep away from sources of ignition. Stop leak if without risk. Absorb with DRY earth, sand or other non-combustible material. Do not get water inside container. Do not touch spilled material. Prevent entry into sewers, basements or confined areas; dike if needed. Call for assistance on disposal. Be careful that the product is not present at a concentration level above TLV. Check TLV on the MSDS and with local authorities.

## Section 7: Handling and Storage

**Precautions:**
Keep away from heat. Keep away from sources of ignition. Ground all equipment containing material. Do not ingest. Do not breathe gas/fumes/ vapor/spray. Wear suitable protective clothing. In case of insufficient ventilation, wear suitable respiratory equipment. If ingested, seek medical advice immediately and show the container or the label. Avoid contact with skin and eyes. Keep away from incompatibles such as oxidizing agents.

**Storage:**
Store in a segregated and approved area. Keep container in a cool, well-ventilated area. Keep container tightly closed and sealed until ready for use. Avoid all possible sources of ignition (spark or flame).

## Section 8: Exposure Controls/Personal Protection

**Engineering Controls:**
Provide exhaust ventilation or other engineering controls to keep the airborne concentrations of vapors below their respective threshold limit value. Ensure that eyewash stations and safety showers are proximal to the work-station location.

**Personal Protection:**
Splash goggles. Lab coat. Vapor respirator. Be sure to use an approved/certified respirator or equivalent. Gloves.

**Personal Protection in Case of a Large Spill:**
Splash goggles. Full suit. Vapor respirator. Boots. Gloves. A self contained breathing apparatus should be used to avoid inhalation of the product. Suggested protective clothing might not be sufficient; consult a specialist BEFORE handling this product.

**Exposure Limits:**
TWA: 200 STEL: 500 CEIL: 300 (ppm) from OSHA (PEL) [United States] TWA: 50 (ppm) from ACGIH (TLV) [United States] SKIN TWA: 100 STEL: 150 from NIOSH [United States] TWA: 375 STEL: 560 (mg/m3) from NIOSH [United States] Consult local authorities for acceptable exposure limits.

## Section 9: Physical and Chemical Properties

**Physical state and appearance:** Liquid.

**Odor:** Sweet, pungent, Benzene-like.

**Taste:** Not available.

**Molecular Weight:** 92.14 g/mole

**Color:** Colorless.

**pH (1% soln/water):** Not applicable.

**Boiling Point:** 110.6°C (231.1°F)

**Melting Point:** -95°C (-139°F)

**Critical Temperature:** 318.6°C (605.5°F)

**Specific Gravity:** 0.8636 (Water = 1)

**Vapor Pressure:** 3.8 kPa (@ 25°C)

**Vapor Density:** 3.1 (Air = 1)

**Volatility:** Not available.

**Odor Threshold:** 1.6 ppm

**Water/Oil Dist. Coeff.:** The product is more soluble in oil; log(oil/water) = 2.7

**Ionicity (in Water):** Not available.

**Dispersion Properties:** See solubility in water, diethyl ether, acetone.

**Solubility:**
Soluble in diethyl ether, acetone. Practically insoluble in cold water. Soluble in ethanol, benzene, chloroform, glacial acetic acid, carbon disulfide. Solubility in water: 0.561 g/l @ 25 deg. C.

## Section 10: Stability and Reactivity Data

**Stability:** The product is stable.

**Instability Temperature:** Not available.

**Conditions of Instability:** Heat, ignition sources (flames, sparks, static), incompatible materials

**Incompatibility with various substances:** Reactive with oxidizing agents.

**Corrosivity:** Non-corrosive in presence of glass.

**Special Remarks on Reactivity:**
Incompatible with strong oxidizers, silver perchlorate, sodium difluoride, Tetranitromethane, Uranium Hexafluoride. Frozen Bromine Trifluoride reacts violently with Toluene at -80 deg. C. Reacts chemically with nitrogen oxides, or halogens to form nitrotoluene, nitrobenzene, and nitrophenol and halogenated products, respectively.

**Special Remarks on Corrosivity:** Not available.

**Polymerization:** Will not occur.

## Section 11: Toxicological Information

**Routes of Entry:** Absorbed through skin. Dermal contact. Eye contact. Inhalation. Ingestion.

**Toxicity to Animals:**
WARNING: THE LC50 VALUES HEREUNDER ARE ESTIMATED ON THE BASIS OF A 4-HOUR EXPOSURE. Acute oral toxicity (LD50): 636 mg/kg [Rat]. Acute dermal toxicity (LD50): 14100 mg/kg [Rabbit]. Acute toxicity of the vapor (LC50): 440 24 hours [Mouse].

**Chronic Effects on Humans:**
CARCINOGENIC EFFECTS: A4 (Not classifiable for human or animal.) by ACGIH, 3 (Not classifiable for human.) by IARC. May cause damage to the following organs: blood, kidneys, the nervous system, liver, brain, central nervous system (CNS).

**Other Toxic Effects on Humans:**
Hazardous in case of skin contact (irritant), of ingestion, of inhalation. Slightly hazardous in case of skin contact (permeator).

**Special Remarks on Toxicity to Animals:**
Lowest Published Lethal Dose: LDL [Human] - Route: Oral; Dose: 50 mg/kg LCL [Rabbit] - Route: Inhalation; Dose: 55000 ppm/40min

**Special Remarks on Chronic Effects on Humans:**
Detected in maternal milk in human. Passes through the placental barrier in human. Embryotoxic and/or foetotoxic in animal. May cause adverse reproductive effects and birth defects (teratogenic). May affect genetic material (mutagenic)

**Special Remarks on other Toxic Effects on Humans:**

Acute Potential Health Effects: Skin: Causes mild to moderate skin irritation. It can be absorbed to some extent through the skin. Eyes: Cauess mild to moderate eye irritation with a burning sensation. Splash contact with eyes also causes conjunctivitis, blepharospasm, corneal edema, corneal abraisons. This usually resolves in 2 days. Inhalation: Inhalation of vapor may cause respiratory tract irritation causing coughing and wheezing, and nasal discharge. Inhalation of high concentrations may affect behavior and cause central nervous system effects characterized by nausea, headache, dizziness, tremors, restlessness, lightheadedness, exhilaration, memory loss, insomnia, impaired reaction time, drowsiness, ataxia, hallucinations, somnolence, muscle contraction or spasticity, unconsciousness and coma. Inhalation of high concentration of vapor may also affect the cardiovascular system (rapid heart beat, heart palpitations, increased or decreased blood pressure, dysrhythmia, ), respiration (acute pulmonary edema, respiratory depression, apnea, asphyxia), cause vision disturbances and dilated pupils, and cause loss of appetite. Ingestion: Aspiration hazard. Aspiration of Toluene into the lungs may cause chemical pneumonitis. May cause irritation of the digestive tract with nausea, vomiting, pain. May have effects similar to that of acute inhalation. Chronic Potential Health Effects: Inhalation and Ingestion: Prolonged or repeated exposure via inhalation may cause central nervous system and cardiovascular symptoms similar to that of acute inhalation and ingestion as well liver damage/failure, kidney damage/failure (with hematuria, proteinuria, oliguria, renal tubular acidosis), brain damage, weight loss, blood (pigmented or nucleated red blood cells, changes in white blood cell count), bone marrow changes, electrolyte imbalances (Hypokalemia, Hypophostatemia), severe, muscle weakness and Rhabdomyolysis. Skin: Repeated or prolonged skin contact may cause defatting dermatitis.

## Section 12: Ecological Information

**Ecotoxicity:**
Ecotoxicity in water (LC50): 313 mg/l 48 hours [Daphnia (daphnia)]. 17 mg/l 24 hours [Fish (Blue Gill)]. 13 mg/l 96 hours [Fish (Blue Gill)]. 56 mg/l 24 hours [Fish (Fathead minnow)]. 34 mg/l 96 hours [Fish (Fathead minnow)]. 56.8 ppm any hours [Fish (Goldfish)].

**BOD5 and COD:** Not available.

**Products of Biodegradation:**
Possibly hazardous short term degradation products are not likely. However, long term degradation products may arise.

**Toxicity of the Products of Biodegradation:** The products of degradation are less toxic than the product itself.

**Special Remarks on the Products of Biodegradation:** Not available.

## Section 13: Disposal Considerations

**Waste Disposal:**
Waste must be disposed of in accordance with federal, state and local environmental control regulations.

## Section 14: Transport Information

**DOT Classification:** CLASS 3: Flammable liquid.

**Identification:** : Toluene UNNA: 1294 PG: II

**Special Provisions for Transport:** Not available.

## Section 15: Other Regulatory Information

**Federal and State Regulations:**
California prop. 65: This product contains the following ingredients for which the State of California has found to cause cancer, birth defects or other reproductive harm, which would require a warning under the statute: Toluene California prop. 65 (no significant risk level): Toluene: 7 mg/day (value) California prop. 65 (acceptable daily intake level): Toluene: 7 mg/day (value) California prop. 65: This product contains the following ingredients for which the State of California has found to cause birth defects which would require a warning under the statute: Toluene Connecticut hazardous material survey.: Toluene Illinois

toxic substances disclosure to employee act: Toluene Illinois chemical safety act: Toluene New York release reporting list: Toluene Rhode Island RTK hazardous substances: Toluene Pennsylvania RTK: Toluene Florida: Toluene Minnesota: Toluene Michigan critical material: Toluene Massachusetts RTK: Toluene Massachusetts spill list: Toluene New Jersey: Toluene New Jersey spill list: Toluene Louisiana spill reporting: Toluene California Director's List of Hazardous Substances.: Toluene TSCA 8(b) inventory: Toluene TSCA 8(d) H and S data reporting: Toluene: Effective date: 10/04/82; Sunset Date: 10/0/92 SARA 313 toxic chemical notification and release reporting: Toluene CERCLA: Hazardous substances.: Toluene: 1000 lbs. (453.6 kg)

**Other Regulations:**
OSHA: Hazardous by definition of Hazard Communication Standard (29 CFR 1910.1200). EINECS: This product is on the European Inventory of Existing Commercial Chemical Substances.

**Other Classifications:**

**WHMIS (Canada):**
CLASS B-2: Flammable liquid with a flash point lower than 37.8°C (100°F). CLASS D-2A: Material causing other toxic effects (VERY TOXIC).

**DSCL (EEC):**
R11- Highly flammable. R20- Harmful by inhalation. S16- Keep away from sources of ignition - No smoking. S25- Avoid contact with eyes. S29- Do not empty into drains. S33- Take precautionary measures against static discharges.

**HMIS (U.S.A.):**

**Health Hazard:** 2

**Fire Hazard:** 3

**Reactivity:** 0

**Personal Protection:** h

**National Fire Protection Association (U.S.A.):**

**Health:** 2

**Flammability:** 3

**Reactivity:** 0

**Specific hazard:**

**Protective Equipment:**
Gloves. Lab coat. Vapor respirator. Be sure to use an approved/certified respirator or equivalent. Wear appropriate respirator when ventilation is inadequate. Splash goggles.

## Section 16: Other Information

**References:** Not available.

**Other Special Considerations:** Not available.

**Created:** 10/10/2005 08:30 PM

**Last Updated:** 05/21/2013 12:00 PM

*The information above is believed to be accurate and represents the best information currently available to us. However, we make no warranty of merchantability or any other warranty, express or implied, with respect to such information, and we assume no liability resulting from its use. Users should make their own investigations to determine the suitability of the information for their particular purposes. In no event shall ScienceLab.com be liable for any claims, losses, or damages of any third party or for lost profits or any special, indirect, incidental, consequential or exemplary damages, howsoever arising, even if ScienceLab.com has been advised of the possibility of such damages.*